

SweetSpot: Near-Infrared Observations of Thirteen Type Ia Supernovae from a New NOAO Survey Probing the Nearby Smooth Hubble Flow

Anja Weyant¹, W. Michael Wood-Vasey¹, Lori Allen², Peter M. Garnavich³, Saurabh W. Jha⁴,
Richard Joyce², Thomas Matheson²

anw19@pitt.edu

November 10, 2018

ABSTRACT

We present 13 Type Ia supernovae (SNe Ia) observed in the restframe near-infrared (NIR) from $0.02 < z < 0.09$ with the WIYN High-resolution Infrared Camera (WHIRC) on the WIYN 3.5-m telescope. With only 1–3 points per light curve and a prior on the time of maximum from the spectrum used to type the object we measure an H -band dispersion of spectroscopically normal SNe Ia of 0.164 mag. These observations continue to demonstrate the improved standard brightness of SNe Ia in H -band even with limited data. Our sample includes two SNe Ia at $z \sim 0.09$, which represent the most distant restframe NIR H -band observations published to date.

This modest sample of 13 NIR SNe Ia represent the pilot sample for “SweetSpot” – a three-year NOAO Survey program that will observe 144 SNe Ia in the smooth Hubble flow. By the end of the survey we will have measured the relative distance to a redshift of $z \sim 0.05$ to 1%. Nearby Type Ia supernova (SN Ia) observations such as these will test the standard nature of SNe Ia in the restframe NIR, allow insight into the nature of dust, and provide a critical anchor for future cosmological SN Ia surveys at higher redshift.

Subject headings: supernova, cosmology

1. Introduction

The discovery of the accelerating expansion of the Universe with Type Ia supernovae (SNe Ia) (Riess et al. 1998; Perlmutter et al. 1999) has sparked a decade-and-a-half of intensive Type Ia

¹ Pittsburgh Particle physics, Astrophysics, and Cosmology Center (PITT PACC). Physics and Astronomy Department, University of Pittsburgh, Pittsburgh PA, 15260

² National Optical Astronomy Observatory, 950 North Cherry Avenue, Tucson, AZ, 85719, USA

³ Department of Physics, 225 Nieuwland Science Hall, Notre Dame, IN, 46556, USA

⁴ Department of Physics and Astronomy, Rutgers, the State University of New Jersey, 136 Frelinghuysen Road, Piscataway, NJ 08854, USA

supernova (SN Ia) studies to pursue the nature of dark energy. High-redshift SN Ia surveys attempt to measure the equation-of-state parameter to sufficiently distinguish among dark energy models. The majority of this work has been focused on standardizing the restframe optical luminosities of SNe Ia. The goal of low-redshift surveys has been to both provide the distance anchor for high-redshift relative distance measurements and to better calibrate SNe Ia as standard candles through improved understanding of SNe Ia themselves.

As the amount of available SN Ia data has grown dramatically, systematic uncertainties have come to dominate cosmological distance measurements with SNe Ia (Albrecht et al. 2006; Astier et al. 2006; Wood-Vasey et al. 2007; Kessler et al. 2009; Sullivan et al. 2010; Conley et al. 2011). A well-established systematic affecting SNe Ia is dust reddening and extinction (see, for example, Jha et al. 2007; Conley et al. 2007; Wang et al. 2006; Goobar 2008; Hicken et al. 2009; Wang et al. 2009; Folatelli et al. 2010; Foley & Kasen 2011; Chotard et al. 2011; Scolnic et al. 2013). It is difficult to separate the effects of reddening as a result of dust from intrinsic variation in the colors of SNe Ia. Unfortunately, most observations of SNe Ia are made in the rest-frame optical and UV where reddening corrections are large.

SNe Ia are superior distance indicators in the near-infrared (NIR),¹ with more standard peak JHK_s magnitudes and relative insensitivity to reddening (Meikle 2000; Krisciunas et al. 2004a, 2007) than in the restframe optical passbands traditionally used in SN Ia distance measurements. Additionally, Krisciunas et al. (2004a) found that objects that are peculiar at optical wavelengths such as SN 1999aa, SN 1999ac, and SN 1999aw appear normal at infrared wavelengths. Although it appears that the 2006bt-like subclass of SNe have normal decline rates and V -band peak magnitudes but display intrinsically-red colors and have broad, slow-declining light curves in the NIR similar to super-Chandra SNe Ia (Foley et al. 2010; Phillips 2012).

These early results have motivated several efforts to pursue large samples of SNe Ia observed in the restframe NIR with 1.3–2.5-m telescopes: CSP-I,II (Contreras et al. 2010; Folatelli et al. 2010; Stritzinger et al. 2011; Kattner et al. 2012); CfA (Wood-Vasey et al. 2008); RAISIN (Kirshner et al. 2012). The results from these projects to date indicate that SNe Ia appear to be *standard* NIR candles to $\lesssim 0.15$ mag (Wood-Vasey et al. 2008; Folatelli et al. 2010; Kattner et al. 2012), particularly in the H band. NIR observations of SNe Ia are a current significant focus of nearby studies of SNe Ia. Recent work by Barone-Nugent et al. (2012) used 8-m class telescopes to observe 12 SNe Ia in the NIR from $0.03 < z < 0.08$ and found promising evidence that the H -band peak magnitude of SNe Ia may have a scatter as small $\sigma_H = 0.085$ mag. This work demonstrated the benefit of using larger-aperture telescopes in overcoming the significantly increased background of the night sky in the NIR.

In this paper we introduce a new effort to observe SNe Ia in the NIR in the nearby smooth Hubble flow. “SweetSpot” is a 72-night, three-year NOAO Survey program (2012B-0500) to observe

¹In this paper we use the term “near-infrared” to refer to observed wavelengths from $1 < \lambda < 2.5 \mu\text{m}$.

SNe Ia in JHK_s using the WIYN 3.5-m telescope and the WIYN High-resolution Infrared Camera (WHIRC). Our goal is to extend the rest-frame H -band NIR Hubble diagram to $z \sim 0.08$ to (1) verify recent evidence that SN Ia are excellent standard candles in the NIR, particularly in the H band; (2) test if the recent correlation between optical luminosity and host galaxy mass holds in the NIR; (3) improve our understanding of intrinsic colors of SNe Ia; (4) study the nature of dust in galaxies beyond our Milky Way; (5) and provide a standard well-calibrated NIR restframe reference for future higher-redshift supernova surveys.

In this paper we present results from our 2011B pilot proposal. In Section 2 we discuss our data reduction and present light curves of 13 SNe Ia. To this sample we add data from the literature (Section 3) and fit the light curves using SNooPy (Burns et al. 2011). Details of how we perform the fitting are discussed in Section 4. We present our results, including an H -band Hubble diagram, in Section 5. We discuss our overall SweetSpot program strategy and goals along with future prospects for restframe H -band SN Ia observations in Section 7, and conclude in Section 8.

2. The Observation and Processing of the SN Ia Sample

2.1. Observations and Sample Selection

We were awarded seven nights of National Optical Astronomy Observatory (NOAO) time in 2011B to image SNe Ia in the NIR using the WIYN 3.5m Observatory at Kitt Peak National Observatory (KPNO) with the WHIRC detector. WHIRC (Meixner et al. 2010) is a NIR imager (0.9–2.5 μm) with a 3.'3 field of view and 0.''1 pixel scale. The combination of WIYN+WHIRC allows us to observe SNe Ia out to a redshift of ~ 0.09 .

Three-and-a-half nights of this time were usable; the rest was lost to bad weather. The light curves presented here thus typically have only 1–3 points in each filter and are sparser than our eventual program goals of 3–10 points per light curve. Our sample (see Table 1) was selected from SNe Ia reported in the IAU Central Bureau for Astronomical Telegrams (CBET)² and The Astronomers Telegram (ATel)³ that were spectroscopically confirmed as Type Ia and were in our preferred redshift range of $0.02 < z < 0.08$.

Our goal is to have the first observation in the light curve within two weeks of maximum. We are focused on the time from 10–20 days after B-band maximum light as the most standard brightness for SNe Ia in the H-band. Our awarded time is typically scheduled around the full moon and therefore spaced 2-3 weeks apart. Additionally, there is a lack of targets at the beginning of the season until searches are up and running. When we combine weather with these factors, we find that about 30% of our light curves from 2011B have their first observation more than 14 days

²<http://www.cbat.eps.harvard.edu/cbet/RecentCBETs.html>

³<http://www.astronomerstelegam.org/>

after maximum.

During the first two semesters of our SweetSpot survey, we have been awarded more nights per semester, more nights occurring later in the semester, and had better weather. Preliminary results show that we are doing significantly better in obtaining earlier light-curve points, with only 10% of our light curves having their first observation more than 14 days after B-band maximum light.

Here we present J - and H -band light curves of the 13 of the 18 SNe Ia that were sufficiently isolated from the background light of their host galaxy. We obtained template images for the other 5 supernovae starting in 2012B during our main NOAO Survey program. The full host-galaxy-subtracted sample will be presented in future work. A summary of the SNe Ia presented in this work can be found in Tables 2 and 3. We describe our data processing in Section 2.2 and photometric analysis and calibration in Section 2.3.

A typical WIYN observation consisted of a 3x3 grid dither pattern with 30'' spacing with a 60 s exposure time at each pointing. For objects or conditions requiring more total exposure time, we typically executed the dither pattern multiple times with a 5'' offset between dither sets. Our observations were conducted in both J and H with priority given to H . We obtained calibration images consisting of a set of 10 dome flats with the flat lamp off and another set with the flat lamp on. We used the WHIRC “high” lamps, which are the standard KPNO MR16 halogen lamps with the reflective surface coated with aluminum by the NOAO coatings lab. We also obtained dark images for monitoring of the dark behavior of the detector, but we do not use these dark images in our analysis.

2.2. Image Processing and Coaddition

The data were reduced in IRAF⁴ following the steps outlined in the WHIRC Reduction Manual (Joyce 2009):

1. The raw images were trimmed of detector reference pixels outside the main imaging area and corrected for the sub-linear response of the array.
2. The ON dome flats were combined; the OFF dome flats were combined; and the OFF combined dome flat was then subtracted from the ON combined dome flat to yield the pixel-by-pixel response.
3. The pupil ghost (an additive artifact resulting from internal reflection within the optical elements of WHIRC) was removed from this response using the IRAF routine `mscred.rmpupil`.

⁴IRAF is distributed by the National Optical Astronomy Observatory, which is operated by the Association of Universities for Research in Astronomy, Inc., under cooperative agreement with the National Science Foundation

4. For each target, the set of dithered science images were used to generate a median-filtered sky frame. The individual science images were then sky-subtracted and flat-fielded using these median frames.
5. The geometric distortion resulting from a difference in plate scales in the x and y coordinates and field distortion at the input to WHIRC was corrected using the IRAF routine `geotran` and the pre-computed WHIRC geometric distortion calibration from 2009 Mar 05⁵.
6. The individual science images were stacked using the IRAF routine `upsqid.xyget` to find the common stars in the images and create a registration database between the individual images in an observation sequence. Intensity offsets were determined from the overlap regions in the registration database and the set of individual images were combined into a composite image using the IRAF routine `upsqid.nircombine`. An exposure map of a typical stacked observation sequence can be found in Fig. 1.

Representative postage stamp images from the processed *H*-band composite images of our supernovae are shown in Fig. 2.

2.3. Photometry and Calibration

We measured the detected counts of the SNe Ia and the stars in the field with aperture photometry on the stacked images using the Goddard Space Flight Center IDL Astronomy User’s Library routines `gcntrd` and `aper`⁶. We used an aperture diameter of 1.5 FWHM (FWHM values were typically around 2”) and measured the background in a surrounding sky annulus from 1.5 FWHM + 0.”1 to 1.5 FWHM + 0.”6. These counts in ADU/(60-second) equivalent exposure were converted to instrumental magnitudes $m_{\text{inst},f} = -2.5 \log_{10} \text{ADU}/60 \text{ sec}$.

To calibrate the instrumental magnitudes we first define a transformation between the WHIRC and the Two Micron All Sky Survey (2MASS; Skrutskie et al. 2006) systems using the following equation

$$m_f^{2\text{MASS}} - m_{\text{inst},f}^{\text{WHIRC}} = \text{zpt}_f + k_f (X - 1) + c_f ((m_J^{2\text{MASS}} - m_H^{2\text{MASS}}) - 0.5 \text{ mag}) \quad (1)$$

where f designates the filter, X is the airmass, and the 2MASS color is compared to a reference of $m_J^{2\text{MASS}} - m_H^{2\text{MASS}} = 0.5 \text{ mag}$, which represents the typical color of stars in our fields as well as SNe Ia after maximum. We then jointly solve for the zeropoint (zpt), airmass coefficient (k)⁷, and

⁵<http://www.noao.edu/kpno/manuals/whirc/datared.html>

⁶<http://idlastro.gsfc.nasa.gov/>

⁷Our sign convention for k means that k should be negative. The opposite convention is also common in the literature.

color coefficient (c) using all instrumental magnitudes measured from 2MASS stars in the fields from our 2011 Nov. 15 and 2012 Jan. 8 nights. This procedure was performed separately for each filter following Eq. 1.

Our fit for each filter is plotted in Fig. 3 and our fit results are summarized in Table 4. We find non-zero color terms of $c_J = 0.062 \pm 0.035$ and $c_H = -0.186 \pm 0.043$ between the 2MASS and WHIRC systems, and airmass coefficients of $k_J = -0.051 \pm 0.020$ mag/airmass and $k_H = -0.066 \pm 0.030$ mag/airmass.

Matheson et al. (2012) used the same WIYN+WHIRC system to observe the very nearby SN 2011fe in M101, and used “canonical” values of $(k_J, k_H, k_{K_s}) = (-0.08, -0.04, -0.07)$ mag/airmass (in our sign convention for k). These values were based on a long-term study of k_J , k_H , and k_K at KPNO in the 1980s using single-channel NIR detectors. This effort found a range of values of $-0.12 < k_J < -0.07$ mag/airmass, $-0.08 < k_H < -0.04$ mag/airmass, and $-0.11 < k_K < -0.07$ mag/airmass with a significant seasonal variation dependent on the precipitable water vapor (R. R. Joyce and R. Probst, private communication). The filters used in these measurements were wider than the standard 2MASS filters or WHIRC filters we use here. The narrow WHIRC filters do not include some of the significant water-vapor absorption regions included in the NIR filters used in the 1980s KPNO study and thus would reasonably be expected to have a smaller absolute value of k_J . Our determined k_J and k_H values are thus consistent with these previous results. However, the variation of k in the NIR as a result of water vapor strongly motivates future improvements in tracking precipitable water vapor and NIR extinction to improve the instantaneous determination of k .

We then selected a star in each field that was near the supernova and had a similar color to the supernova at the time of our observations. These reference stars are listed in Table 5. We used the best observation of the reference star, our fit results from Table 4, and Eq. 1 to create a list of calibrated standard stars in the WHIRC natural system. We note that our only observation of SN 2011io was taken under partial clouds. For a given field, the standard star was then used to find the zeropoint for each stacked image as follows

$$\text{zpt}_{f,i} = m_{\text{cal},f}^{\text{WHIRC}} - m_{\text{inst},f,i}^{\text{WHIRC}} \quad (2)$$

where the i subscript indicates stacked image and m_{cal} is the calibrated standard star for that field. This zeropoint was then applied to the measured instrument magnitude from the supernovae to generate the calibrated supernova magnitude in the WHIRC natural system. These light curves are presented in Table 6.

We report magnitudes in the WIYN+WHIRC natural system.⁸

⁸For reference, the filter transmissions for WIYN+WHIRC can be found at <http://www.noao.edu/kpno/manuals/whirc/filters.html>

3. SN Ia Sample from the Literature

To our sample of WHIRC SNe Ia we add the following data from the literature:

- A compilation of 23 SNe Ia from Jha et al. (1999), Hernandez et al. (2000), Krisciunas et al. (2000), Krisciunas et al. (2004a), Krisciunas et al. (2004b), Phillips et al. (2006), Pastorello et al. (2007b), Pastorello et al. (2007a), and Stanishev et al. (2007). This is the same set that was used as the “literature” sample by Wood-Vasey et al. (2008). We use 22 SNe Ia from this set, one of which was observed by the Carnegie Supernova Project (CSP). We refer to the 21 SNe Ia that are unique to this sample as K+ in recognition of the substantial contributions by Kevin Krisciunas to this sample and the field of NIR SNe Ia.
- Wood-Vasey et al. (2008) presented JHK_s measurements of 21 SNe Ia from the Center for Astrophysics (CfA) Supernova Program using the robotic 1.3 m Peters Automated Infrared Imaging Telescope (PAIRITEL; Bloom et al. 2006) at Mount Hopkins, Arizona. We use 17 SNe Ia from this sample which we refer to as WV08.
- Contreras et al. (2010) and Stritzinger et al. (2011) present 69 SNe Ia from the CSP using observations at the Las Campanas Observatory in Chile (Hamuy et al. 2006). The CSP observations in $YJHK_s$ were carried out with the Wide Field Infrared Camera (WIRC) attached to the du Pont 2.5 m Telescope and RetroCam on the Swope 1-m telescope supplemented by occasional imaging with the PANIC NIR imager (Osip et al. 2004) on the Magellan Baade 6.5-m telescope. We use 55 SNe Ia from this sample, 6 of which are also in WV08. We refer to the 49 SNe Ia that were not observed by Wood-Vasey et al. (2008) as CSP.
- Barone-Nugent et al. (2012) extended the rest-frame NIR sample out to $z \sim 0.08$ with 12 SNe Ia observed in JH on Gemini Observatory’s 8.2m Gemini North with the NIR Imager and Spectrometer (Hodapp et al. 2000) and on ESO’s 8.1m VLT using HAWK-I (Casali et al. 2006). We use these 12 SNe Ia and refer to this set as BN12.

To arrive at these samples we removed supernovae that were reported to have a spectrum similar to the sub-luminous SN 1991bg (SN 2006bd, SN 2007N, SN 2007ax, SN 2007ba, SN 2009F); were reported to have a spectrum that was peculiar (SN 2006bt, SN 2006ot); were identified as possible super-Chandrasekhar mass objects (SN 2007if, SN 2009dc); were determined to be highly reddened (SN 1999cl, SN 2003cg, SN 2005A, SN 2006X); or were found to have a decline rate parameter $\Delta m_{15} > 1.7$ (SN 2005bl, SN 2005ke, SN 2005ku, SN 2006mr) according to the information provided in Folatelli et al. (2010); Contreras et al. (2010); Stritzinger et al. (2011); Burns et al. (2011). We also removed SN 2002cv that Elias-Rosa et al. (2008) find to be heavily obscured and SN 2007hx whose photometry is unreliable (Maximilian Stritzinger, private communication). A redshift histogram of this entire sample, which represents the currently available collection of published normal NIR SNe Ia, is plotted in Fig. 4. Note that with WIYN+WHIRC we can reach out to $z \sim 0.09$ and cover the entirety of the nearby smooth Hubble flow from $0.03 < z < 0.08$.

We used the quoted system transmission function reported by each survey. For SNe Ia that were observed by multiple surveys, we fit all of the available photometry for the SN Ia.

4. Analysis

We fit the light-curves using the suite of supernova analysis tools developed by CSP called SNooPy (Burns et al. 2011). We fit the data using SNooPy (version 2.0-267) “max_model” fitting that uses the following model m_X :

$$m_X(t - t_{\max}) = T_Y((t' - t_{\max})/(1 + z), \Delta m_{15}) + m_Y + R_X E(B - V)_{\text{Gal}} + K_{X,Y}(z, (t' - t_{\max})/(1 + z), E(B - V)_{\text{host}}, E(B - V)_{\text{Gal}}) \quad (3)$$

where t is time in days in the observer frame, T_Y is the SNooPy light-curve template, m_Y is the peak magnitude in filter Y, t_{\max} is the time of maximum in the B band, Δm_{15} is the decline rate parameter (Phillips 1993), $E(B - V)_{\text{Gal}}$ and $E(B - V)_{\text{host}}$ are the reddening resulting from the Galactic foreground and the host galaxy, R_X is the total-to-selective absorption for filters X , and $K_{X,Y}$ is the cross-band K-correction from rest-frame X to observed Y. The free parameters in this model are t_{\max} , Δm_{15} , and m_Y . We do not assume any relationship between the different filters and therefore do not apply any color correction. We generate the template $T(t, \Delta m_{15})$ from the code of Burns et al. (2011) which generates rest-frame templates for J and H from the CSP data (Folatelli et al. 2010).

We use SNooPy to perform the K-corrections on all of the data using the Hsiao et al. (2007) spectral templates. We do not warp or “mangle” the spectral template to match the observed color when performing the K-corrections. A simpler approach makes sense as we are interested in measuring the peak brightness using one NIR band and a prior on t_{\max} . In Fig. 5 we plot the H -band filter transmission for the different surveys in our sample. Overlaid are synthetic spectra at various redshifts. Note the difference in widths and up to $0.05 \mu\text{m}$ shift in the positions of the blue and red edges of the different H -band filters. While SNe Ia are standard in their rest-frame H -band brightness, there is a significant feature at $1.8 \mu\text{m}$ which moves longward of the red edge of the H -band filter quickly from just $z = 0$ to $z = 0.05$. This feature means that it is quite important to have well-understood transmission functions and spectral templates. However, given that the main effect is the feature moving across the edge of the filter cutoff, knowing the filter bandpass provides most of the necessary information without an immediate need for a full system transmission function.

For the 2011B data presented in this paper t_{\max} is fixed to an estimate measured from the spectrum as reported in the ATels/CBETs. This significant prior is necessary as our NIR data only have a few points per light curve (see Table 2), which are not enough to independently estimate t_{\max} . We also fix the light-curve width parameter to $\Delta m_{15} = 1.1$. This is reasonable as we have already eliminated SNe Ia spectroscopically identified as 91bg-like from observation in our own

program and from consideration when including the current literature sample. As a result of these priors, only the peak magnitude in each filter (JH) is determined from fitting the light curve (see Table 3). The quoted peak magnitude uncertainties are then determined from least-squares fitting. The light-curve fits to each of the new SNe Ia presented here are shown in Fig. 6.

In order to use a consistent method to compare the apparent brightness of the SNe Ia across our entire sample we applied a similar process for the literature sample. We use a prior on the time of maximum for the K+, CSP, and WV08 data from the SNooPy fit to the B -band light curve alone and fixed $\Delta m_{15} = 1.1$. SN 2005ch is an exception as we do not have a B -band light curve. We fixed the time of maximum for this SN to an estimate from the spectrum reported in Dennefeld & Riquebourg (2005). The optical light curves are not available for the BN12 data and not all SNe Ia in this sample were reported in ATels. We cannot estimate t_{\max} for a fixed value of Δm_{15} as we have done for the other samples. Therefore, we fixed the time of maximum and stretch to that reported for these SNe Ia in Maguire et al. (2012).

The peak apparent magnitude for the 2011B SNe Ia in JH are listed in Table 3. A summary of the light curve fit parameters - which includes the peak apparent magnitude - for the CSP, WV08, BN12, and the present W13 samples can be found in Table 7. The W13 data is the same as that in Table 3, but we include it in Table 7 for the convenience of presenting all of the Hubble Diagram information in a single table.

5. Results

5.1. Near-Infrared SN Ia Hubble Diagram

An H -band Hubble diagram for our entire sample is presented in Fig. 7. The recession velocities are based on Virgo infall model of Mould et al. (2000) (see Table 7). For SNe Ia within 3000 km s^{-1} we fix the redshifts to those summarized in Wood-Vasey et al. (2008). The solid line in the top panel of Fig. 7 represents the observed apparent magnitude assuming a standard flat cosmology of $\Omega_M = 0.28$ and $H_0 = 72 \text{ km s}^{-1} \text{ Mpc}^{-1}$ and $M_H = -18.32 \text{ mag}$ (see Section 5.2). The residuals with respect to this line are plotted in the bottom panel. The highest redshift outlier from CSP is SN 2005ag at $z = 0.08062$. Folatelli et al. (2010) find SN 2005ag to be a slow-decliner and therefore more luminous than a normal SN Ia although the luminosity versus decline-rate relationship should correct for this. They also believe that this SN was at the detection limit of LOSS such that Malmquist bias could explain its over-brightness.

We plot the distribution of residuals for each sub-sample in Fig. 8 for the entire set (hatched) and for $z > 0.02$ (solid). The standard deviation of the residuals, σ , for each sample and for the subsample with $z > 0.02$ is given in each subpanel. One can clearly see the smaller spread in the BN12 and W13 samples, a benefit of a higher redshift sample with reduced peculiar velocity uncertainty and photometric uncertainty.

We find a dispersion for our W13 sample of $\sigma_H = 0.227$ mag which reduces to $\sigma_H = 0.164$ mag when we exclude SN 2011hr. SN 2011hr is 91T-like and could be expected to be over-luminous. The dispersion is further reduced to $\sigma_H = 0.138$ mag if we exclude all SN with only one H -band observation and SN 2011hr which leaves us with 8 SNe Ia.

5.2. Absolute H -Band Magnitude of a SN Ia

We find the absolute H -band magnitude M_H by calculating the weighted mean of the difference between the peak apparent magnitude and the distance modulus evaluated at the corresponding redshift assuming a standard flat Λ CDM cosmology of $\Omega_M = 0.28$ and $H_0 = 72$ km s⁻¹ Mpc⁻¹. The weight includes the additional uncertainty as a result of redshift uncertainty associated with a peculiar velocity of 150 km s⁻¹ (Radburn-Smith et al. 2004). We find $M_H = -18.314 \pm 0.024$ mag for the entire sample. This value is completely degenerate with the choice of H_0 , in the sense that a larger H_0 corresponds to a fainter absolute magnitude. So in more generality we find $M_H = (-18.314 \pm 0.024) + 5 \log_{10} (H_0 / (72 \text{ km s}^{-1} \text{ Mpc}^{-1}))$ mag.

If we analyze the measured peak H -band absolute magnitude separately for each sample we find: -18.449 ± 0.056 mag for K+, -18.376 ± 0.040 mag for CSP, -18.317 ± 0.059 mag for WV08, -18.224 ± 0.028 mag for BN12, and -18.375 ± 0.066 mag for W13 (assuming the same $\Omega_M = 0.28$, $H_0 = 72$ km s⁻¹ Mpc⁻¹ Λ CDM cosmology). Note that the uncertainties quoted here are the standard error (i.e., the uncertainty in the determination of the mean) rather than the standard deviation of the distribution around these absolute magnitudes (see Fig. 8). The peak magnitude uncertainty quoted for each SN Ia is underestimated for at least two reasons: (1) SNooPy only returns the statistical uncertainty from fitting and does not include any systematic uncertainties⁹ and (2) the time of maximum is fixed such that uncertainty in the time of maximum is not propagated to the uncertainty in peak magnitude. As a result, we cannot calculate the uncertainty in measured peak H -band absolute magnitude as the uncertainty in the weighted mean. This would underestimate the error in M_H . Instead we look at the spread of the distribution of residuals as a whole to estimate the uncertainty and thus quote the standard error (σ_H / \sqrt{N}).

We consider a worst-case scenario to estimate the maximal contribution of uncertainty in t_{\max} to the uncertainty in M_H by coherently shifting t_{\max} for the entire sample by the uncertainty in t_{\max} . Excluding for a moment the W13 sample for which we do not have an estimate of the t_{\max} uncertainty, we find that M_H shifts by 0.0017 mag indicating that the contribution from t_{\max} uncertainty is negligible. If we assume an uncertainty of ± 2 days for the W13 sample we find a shift of 0.059 mag in the peak absolute brightness. This means for our sample of 12 SN Ia, the maximal contribution of t_{\max} uncertainty to our estimate for M_H is $0.059 / \sqrt{12} = 0.017$ mag.”

To examine the error in M_H incurred by fixing Δm_{15} we refit the WV08, CSP, and K+ B -band

⁹For a list of systematic uncertainties that SNooPy fails to report see Section 4.4 of (Burns et al. 2011).

light curves allowing t_{\max} and Δm_{15} to float. We then use this t_{\max} and Δm_{15} as fixed priors when fitting the JH -band light curves. We find shifts in the measured peak H -band absolute magnitude of -0.031 mag, 0.019 mag, and -0.007 mag for the CSP, K+ and WV08 samples. These are well within our uncertainty on the measured peak apparent magnitude for each sample. Additionally, we find a negligible change in the χ^2 per degree of freedom between the two approaches and thus conclude that we are justified in using the simpler light-curve model.

6. Discussion

6.1. NIR SN Ia as Standard Candles

The dispersion of our W13 sample excluding SN 2011hr ($\sigma_H = 0.164$ mag) is comparable to that of Wood-Vasey et al. (2008) who find an RMS of 0.16 mag in H and Folatelli et al. (2010) who find an RMS of 0.19 mag in H when not correcting for host galaxy extinction. Similar to our analysis, neither result makes a correction to the absolute magnitude according to the decline-rate.

Barone-Nugent et al. (2012) estimate that 1–2 points per light curve should yield a dispersion between 0.096 and 0.116 mag. However, these results derive from a sample with B -band stretch values ranging from 0.8 to 1.15. Greater diversity in our sample is one possible explanation for our larger measured dispersion. Our measured dispersion may be higher because most of our data is from +10 days after maximum and we have no pre-maximum data. Additionally, the times of maximum for our sample came from spectroscopic observations as reported in ATels and CBETs. Spectroscopic phase determination are only precise to ± 2 days (Blondin & Tonry 2007) and there is potentially the equivalent of a couple of days of additional scatter from quick at-the-telescope reductions.

It is possible that the spectroscopic classification and reporting of the time of B -band is systematically biased in some way. For example, while some groups report precisely the best fit spectrum used to type the object and estimate the phase, others merely state the phase as, e.g., “near maximum” or “several days after maximum.” We examined the implications of the extreme case of a coherent bias on t_{\max} for the W13 estimate of M_H by adding and subtracting 2 days to the prior on the time of maximum to *all* W13 SNe Ia. We found that systematically shifting the time of maximum results in a shift of about $+0.06$ mag for $+2$ days and -0.06 mag for -2 days in M_H . This coherent shift in apparent magnitude for the W13 sample is because all of our data are post-maximum light where the SNe Ia are generally fading rather than increasing in brightness.

We also note that the SNe Ia which comprise the W13 sample are not drawn from the faint limits of their discovery surveys. Therefore, Malmquist bias is unlikely to be a problem with the W13 sample.

Our analysis shows that for a set of spectroscopically normal SNe Ia using limited NIR data and a simplified light curve model which does not rely on any optical or stretch information, but rather

only a prior on the time of maximum, we find an observed RMS of 0.164 mag that is comparable to detailed lightcurves from optical-only surveys.

6.2. Absolute Brightness

Our measurement of the absolute brightness for the CSP-sample is in good agreement with the literature. Our CSP-sample results are 0.056 mag dimmer than those of Kattner et al. (2012) who find $M_H = -18.432 \pm 0.017$ mag for their CSP sample of 27 well-observed NIR light curves. The Kattner et al. (2012) analysis included a decline-rate correction. Folatelli et al. (2010) find $M_H = -18.40 \pm 0.08$ using the first set of CSP data and including no decline-rate correction, which is only 0.024 mag brighter than our analysis of the full CSP sample including up through Stritzinger et al. (2011).

We are in slight disagreement with Barone-Nugent et al. (2012) at the 1.5σ level who find $M_H = -18.30 \pm 0.04$ mag as the median absolute magnitude for their sample.¹⁰

We also note that while our measurements for M_H for W13, K+, CSP, and WV08 are in good agreement with each other, W13 and WV08 are in slight disagreement with the BN12 sample ($\sim 2\sigma$) and K+ and CSP are in poor agreement with the BN12 sample ($+3\sigma$). Our treatment of the BN12 sample is different as we do not have access to the optical light curves. We did not determine t_{\max} for a fixed value of stretch as we did for the other samples, but instead used the quoted t_{\max} and stretch from Maguire et al. (2012) as was used in Barone-Nugent et al. (2012). This inconsistent treatment of this sample may be part of the discrepancy with the results of other samples. To test this, we reran the analysis on the BN12 data fixing the decline-rate parameter to $\Delta m_{15} = 1.1$ and allowing the time of maximum to float. We found $M_H = -18.248 \pm 0.030$ mag which is a marginal improvement in agreement. We speculate that additional disagreement here is caused by differences in the SNooPY (Burns et al. 2011) and FLIRT (Mandel et al. 2009) light-curve fitters.

7. SweetSpot: A 3-Year Survey Program with WHIRC

Building off the pilot program presented in this paper, we are currently engaged in a 3-year 72-night large-scale NOAO Survey (2012B-0500; PI: W. M. Wood-Vasey) program to image SNe Ia in the NIR using WIYN+WHIRC. Our goal is to observe ~ 150 spectroscopically confirmed nearby SNe Ia in the NIR using WHIRC. We will obtain a total sample of ~ 150 SN Ia light curves sampled in JH with 3–6 observations per light curve for the bulk of the sample and a subset of 25 SNe Ia observed in JHK_s out to late phases ($> +30$ days) with 6–10 observations per supernova. If

¹⁰For this comparison we have adjusted the originally reported M_H values of Barone-Nugent et al. (2012) to match the common scale of $H_0 = 72 \text{ km s}^{-1} \text{ Mpc}^{-1}$ used in this present analysis and in Folatelli et al. (2010) and Kattner et al. (2012).

SNe Ia are standard in the NIR with to $\sigma_H = 0.1$ mag with no significant systematic bias then 150 SNe Ia in the nearby Hubble flow will allow us to make an overall relative distance measurement to $z \sim 0.05$ to 1%. Alternatively, we will be able to probe systematics at the few percent level, beyond what we are able to do today in the optical due to the significant confusion from host galaxy dust extinction and greater dispersion in the SN Ia optical luminosities.

We continue to rely on the hard work of several nearby supernovae surveys to discover and spectroscopically-confirm the SNe Ia we observe. Specifically, we follow announcements from the IAU/CBETs and ATels of supernovae discovered and/or classified by KAIT/LOSS (Filippenko et al. 2001), CRTS (Drake et al. 2009) surveys, the intermediate Palomar Transient Factory¹¹, Robotic Optical transient search experiment¹², the Backyard Observatory Supernova Search¹³, the Italian Supernova Search Project¹⁴, the La Silla Quest survey¹⁵ (Baltay et al. 2012), the CfA Supernova Group¹⁶(Hicken et al. 2012), the Public ESO Spectroscopic Survey of Transient Objects¹⁷, the Padova-Asiago Supernova Group¹⁸, and the Nearby Supernova Factory II¹⁹(Aldering et al. 2002).

We would be happy to work on collaborative efforts to analyze the SNe Ia we are observing with those who have optical lightcurves and spectra or other near-infrared data and invite those interested to contact the first two authors (AW and MWV) to pursue such opportunities.

With this sample we will extend the SNe Ia NIR H -band Hubble Diagram out to $z \sim 0.08$. This will increase the currently published sample size in this “sweet spot” redshift range by a factor of five. The Carnegie Supernova Project II²⁰ is currently engaged in a similar effort to obtain optical+NIR imaging and spectroscopy for a similar sample size in this same redshift range.

While we will obtain 6–10 light curve observations for most of the SNe Ia, we will also explore constructing the “minimal” H -band Hubble diagram. NIR observations are expensive to take from the ground as a result of the significant emission and absorption from the atmosphere, and expensive from space due to the cryogenic detectors often desired. If we could determine distances reliably with just a few NIR data points combined with an optical light curve, we would significantly increase

¹¹<http://ptf.caltech.edu/iptf/>

¹²<http://www.rotse.net>

¹³<http://bosssupernova.com>

¹⁴<http://italiansupernovae.org>

¹⁵<http://hep.yale.edu/lasillaquest>

¹⁶<http://www.cfa.harvard.edu/supernova/SNgroup.html>

¹⁷<http://www.pessto.org/pessto/index.py>

¹⁸<http://graspa.oapd.inaf.it>

¹⁹<http://snfactory.lbl.gov>

²⁰<http://csp2.lco.cl/>

the number of SN Ia distances that could be measured for a given investment of NIR telescope time. We will realistically evaluate this “minimal” required contribution of NIR data to SN Ia cosmology by analyzing the optical light curve with only one or two H -band observations near maximum and check this against the luminosity distance determined from the actual full H -band light curve. The optical light curve will give us the phase and we will measure the brightness in the near infrared. If this approach is successful it opens the window to exploring SNe Ia at higher redshift even given the significant cost of rest-frame NIR observations. We will quantify the improvement of adding 1–3 NIR observations per SN Ia and make recommendations for the most feasible and beneficial strategy for improving SN Ia cosmology.

If modest observations of only a few restframe H -band points along the lightcurves of a SNe Ia are sufficient to provide a robust and relatively precise distance measurement, then there is significant potential in supplementing future large ground-based surveys, such as the Large Synoptic Survey Telescope (LSST Science Collaborations et al. 2009), with space-based resources such as the James Webb Space Telescope²¹ to obtain restframe H -band observations to check systematic effects in these large surveys and to independently obtain reliable NIR distances to $z > 0.5$.

A newly identified systematic affecting inferred optical luminosity distances from SNe Ia is the stellar mass of the host galaxy (Kelly et al. 2010; Lampeitl et al. 2010; Sullivan et al. 2010; Gupta et al. 2011; Childress et al. 2013). These analyses show that, after light-curve shape corrections, SNe Ia in high-stellar-mass galaxies are found to be 0.1 mag brighter in rest-frame B than in low-stellar-mass galaxies. Recent work based on IFU observations of the local (1 kpc) environments of SNe Ia (Rigault et al. 2013) explains this effect as a consequence of the distribution of *local* star-formation conditions in nearby galaxies. They find that a population of SNe Ia in locally passive environments is 0.2 mag brighter than SNe Ia in locally star-forming environments. In higher-mass galaxies, there is an equal mix of these SNe Ia, leading to a 0.1 mag bias, while in lower-mass galaxies ($M_{\odot} < 10^{9.5}$) such a bright population does not appear to exist.

The NIR photometry we will obtain of the SN host galaxies will provide both reference templates for the supernova lightcurves as well as key observations to determine stellar mass. We will explore if these mass and environmental correlations hold in the near infrared by combining our NIR supernova observations with samples from the literature together with observations of the host galaxies.

We will finally examine the late time color evolution of SNe Ia in the near infrared. SNe Ia have a uniform optical color evolution starting around 30 days past maximum light (Lira 1996; Phillips et al. 1999). The full decay rate and color evolution from maximum light to 100 days will provide excellent calibration of the intrinsic color and dust extinction in SNe Ia. If SNe Ia are confirmed to be standard in their NIR late-time color evolution then we can use a combined UV, optical, and NIR data set to make detailed measurements of the dust extinction in the SN Ia host

²¹<http://www.jwst.nasa.gov/>

galaxies.

8. Conclusion

We are using the WIYN 3.5m Observatory at Kitt Peak as part of an approved NOAO Survey to image nearby SN Ia in the NIR using WHIRC. In this paper we have presented 13 light curves for SNe Ia observed in 2011B as part of this program. Within this set we have contributed 12 new standard SNe Ia to the current nearby NIR sample out to $z \sim 0.09$.

We have presented an updated H -band Hubble diagram including the latest samples from the literature. Considering that we have late-time sparsely sampled lightcurves and a time of maximum that is accurate to a few days, it is remarkable that we measure a dispersion of our sample to be 0.164 mag when excluding 91T-like SN 2011hr. With future semesters of observing and a larger sample of SN Ia observed near maximum, we expect the dispersion to decrease as a result of more comprehensive temporal sampling. The dispersion will also improve as the optical counterparts of these SN Ia become available and the times of maximum can be more accurately determined.

The observations presented in this paper came from NOAO time on WIYN under proposal ID 2011B-0482. AW and MWV were supported in part by NSF AST-1028162. A.W. additionally acknowledges support from PITT PACC and the Zaccheus Daniel Foundation. Supernova research at Rutgers University is supported in part by NSF CAREER award AST-0847157 to SWJ. The “Latest Supernovae” website²² maintained by David Bishop was helpful in planning and executing these observations. We thank Chris Burns for his significant assistance in using SNooPy. We thank Sandhya Rao for her assistance with IRAF. We thank the staff of KPNO and the WIYN telescope and engineering staff for their efforts that enabled these observations. We thank the Tohono O’odham Nation for leasing their mountain to allow for astronomical research. We thank the Aspen Center for Physics for hosting the 2010 summer workshop on “Taking Supernova Cosmology into the Next Decade” where the original discussions that led to the SweetSpot survey took place.

This research has made use of the NASA/IPAC Extragalactic Database (NED) which is operated by the Jet Propulsion Laboratory, California Institute of Technology, under contract with the National Aeronautics and Space Administration.

This publication makes use of data products from the Two Micron All Sky Survey, which is a joint project of the University of Massachusetts and the Infrared Processing and Analysis Center/California Institute of Technology, funded by the National Aeronautics and Space Administration and the National Science Foundation.

Facility: WIYN

²²<http://www.rochesterastronomy.org/supernova.html>

REFERENCES

- Abazajian, K., Adelman-McCarthy, J. K., Agüeros, M. A., et al. 2003, *AJ*, 126, 2081
- . 2005, *AJ*, 129, 1755
- Albrecht, A., Bernstein, G., Cahn, R., et al. 2006, *ArXiv Astrophysics e-prints*, arXiv:astro-ph/0609591, arXiv:astro-ph/0609591
- Aldering, G., Adam, G., Antilogus, P., et al. 2002, in *SPIE Conference Series*, Vol. 4836, *SPIE Proc.*, ed. J. A. Tyson & S. Wolff, 61–72
- Astier, P., Guy, J., Regnault, N., et al. 2006, *A&A*, 447, 31
- Balam, D. D., Graham, M. L., Hsiao, E. Y., & Green, D. W. E. 2011, *Central Bureau Electronic Telegrams*, 2825, 2
- Balanutsa, P., & Lipunov, V. 2011, *Central Bureau Electronic Telegrams*, 2931, 1
- Baltay, C., Rabinowitz, D., Hadjiyska, E., et al. 2012, *The Messenger*, 150, 34
- Barone-Nugent, R. L., Lidman, C., Wyithe, J. S. B., et al. 2012, *MNRAS*, 425, 1007
- Blondin, S., & Tonry, J. L. 2007, *ApJ*, 666, 1024
- Bloom, J. S., Starr, D. L., Blake, C. H., Skrutskie, M. F., & Falco, E. E. 2006, in *Astronomical Society of the Pacific Conference Series*, Vol. 351, *Astronomical Data Analysis Software and Systems XV*, ed. C. Gabriel, C. Arviset, D. Ponz, & S. Enrique, 751
- Bottinelli, L., Durand, N., Fouque, P., et al. 1993, *A&AS*, 102, 57
- Burns, C. R., Stritzinger, M., Phillips, M. M., et al. 2011, *AJ*, 141, 19
- Casali, M., Pirard, J.-F., Kissler-Patig, M., et al. 2006, in *SPIE Conference Series*, Vol. 6269, *SPIE Proc.*
- Childress, M., Aldering, G., Antilogus, P., et al. 2013, *ApJ*, 770, 108
- Chotard, N., Gangler, E., Aldering, G., et al. 2011, *A&A*, 529, L4+
- Conley, A., Carlberg, R. G., Guy, J., et al. 2007, *ApJ*, 664, L13
- Conley, A., Guy, J., Sullivan, M., et al. 2011, *ApJS*, 192, 1
- Contreras, C., Hamuy, M., Phillips, M. M., et al. 2010, *AJ*, 139, 519
- Cox, L., Newton, J., Puckett, T., et al. 2011, *Central Bureau Electronic Telegrams*, 2939, 1

- de Vaucouleurs, G., de Vaucouleurs, A., Corwin, Jr., H. G., et al. 1991, Third Reference Catalogue of Bright Galaxies. Volume I: Explanations and references. Volume II: Data for galaxies between 0^h and 12^h . Volume III: Data for galaxies between 12^h and 24^h . (Springer, New York, NY (USA))
- Dennefeld, M., & Ricquebourg, F. 2005, IAU Circ., 8541, 4
- Drake, A. J., Djorgovski, S. G., Mahabal, A., et al. 2009, ApJ, 696, 870
- . 2011, Central Bureau Electronic Telegrams, 2838, 1
- Elias-Rosa, N., Benetti, S., Turatto, M., et al. 2008, MNRAS, 384, 107
- Falco, E. E., Kurtz, M. J., Geller, M. J., et al. 1999, PASP, 111, 438
- Filippenko, A. V., Li, W. D., Treffers, R. R., & Modjaz, M. 2001, in Astronomical Society of the Pacific Conference Series, Vol. 246, IAU Colloq. 183: Small Telescope Astronomy on Global Scales, ed. B. Paczynski, W.-P. Chen, & C. Lemme, 121
- Fisher, K. B., Huchra, J. P., Strauss, M. A., et al. 1995, ApJS, 100, 69
- Fixsen, D. J., Cheng, E. S., Gales, J. M., et al. 1996, ApJ, 473, 576
- Folatelli, G., Phillips, M. M., Burns, C. R., et al. 2010, AJ, 139, 120
- Foley, R. J., & Kasen, D. 2011, ApJ, 729, 55
- Foley, R. J., Narayan, G., Challis, P. J., et al. 2010, ApJ, 708, 1748
- Fraser, M., Magill, L., Smartt, S., & Kotak, R. 2011, Central Bureau Electronic Telegrams, 2931, 2
- Gal-Yam, A., Yaron, O., Ben-Ami, S., et al. 2011a, The Astronomer’s Telegram, 3798, 1
- Gal-Yam, A., Ben-Ami, S., Yaron, O., et al. 2011b, The Astronomer’s Telegram, 3739, 1
- Goobar, A. 2008, ApJ, 686, L103
- Gupta, R. R., D’Andrea, C. B., Sako, M., et al. 2011, ApJ, 740, 92
- Hamuy, M., Folatelli, G., Morrell, N. I., et al. 2006, PASP, 118, 2
- Hernandez, M., Meikle, W. P. S., Aparicio, A., et al. 2000, MNRAS, 319, 223
- Hicken, M., Wood-Vasey, W. M., Blondin, S., et al. 2009, ApJ, 700, 1097
- Hicken, M., Challis, P., Kirshner, R. P., et al. 2012, ApJS, 200, 12
- Hodapp, K.-W., Hora, J., Graves, E., et al. 2000, in SPIE Conference Series, Vol. 4008, SPIE Proc., ed. Iye, M. and Moorwood, A. F., 1334–1341

- Howerton, S., Drake, A. J., Djorgovski, S. G., et al. 2011, Central Bureau Electronic Telegrams, 2881, 1
- Hsiao, E. Y., Conley, A., Howell, D. A., et al. 2007, ApJ, 663, 1187
- Jha, S., Riess, A. G., & Kirshner, R. P. 2007, ApJ, 659, 122
- Jha, S., Garnavich, P. M., Kirshner, R. P., et al. 1999, ApJS, 125, 73
- Jin, Z., & Gao, X. 2011, Central Bureau Electronic Telegrams, 2871, 1
- Jin, Z., Gao, X., Brimacombe, J., Noguchi, T., & Nakano, S. 2011, Central Bureau Electronic Telegrams, 2825, 1
- Jones, D. H., Read, M. A., Saunders, W., et al. 2009, MNRAS, 399, 683
- Joyce, D. 2009, WIYN High-Resolution Infrared Camera (WHIRC) Quick Guide to Data Reduction Version 1.03, Tech. rep., National Optical Astronomy Observatory
- Karachentsev, I. D., & Makarov, D. A. 1996, AJ, 111, 794
- Kattner, S., Leonard, D. C., Burns, C. R., et al. 2012, PASP, 124, 114
- Kelly, P. L., Hicken, M., Burke, D. L., Mandel, K. S., & Kirshner, R. P. 2010, ApJ, 715, 743
- Kessler, R., Becker, A. C., Cinabro, D., et al. 2009, ApJS, 185, 32
- Kirshner, R. P., et al. 2012, HST Proposal
- Krisciunas, K., Hastings, N. C., Loomis, K., et al. 2000, ApJ, 539, 658
- Krisciunas, K., Phillips, M. M., & Suntzeff, N. B. 2004a, ApJ, 602, L81
- Krisciunas, K., Phillips, M. M., Suntzeff, N. B., et al. 2004b, AJ, 127, 1664
- Krisciunas, K., Garnavich, P. M., Stanishev, V., et al. 2007, AJ, 133, 58
- Lampeitl, H., Smith, M., Nichol, R. C., et al. 2010, ApJ, 722, 566
- Lipunov, V., & Balanutsa, P. 2011, Central Bureau Electronic Telegrams, 2873, 1
- Lira, P. 1996, Master's thesis, MS thesis. Univ. Chile (1996)
- LSST Science Collaborations, Abell, P. A., Allison, J., et al. 2009, ArXiv e-prints, 0912.0201, arXiv:0912.0201
- Maguire, K., Sullivan, M., Ellis, R. S., et al. 2012, MNRAS, 426, 2359
- Mandel, K. S., Wood-Vasey, W. M., Friedman, A. S., & Kirshner, R. P. 2009, ApJ, 704, 629

- Marion, G. H. 2011, Central Bureau Electronic Telegrams, 2838, 3
- Marion, G. H., & Berlind, P. 2011a, Central Bureau Electronic Telegrams, 2880, 2
- . 2011b, Central Bureau Electronic Telegrams, 2892, 3
- . 2011c, Central Bureau Electronic Telegrams, 2939, 2
- Matheson, T., Joyce, R. R., Allen, L. E., et al. 2012, ApJ, 754, 19
- Meikle, W. P. S. 2000, MNRAS, 314, 782
- Meixner, M., Smee, S., Doering, R. L., et al. 2010, PASP, 122, 451
- Mould, J. R., Huchra, J. P., Freedman, W. L., et al. 2000, ApJ, 529, 786
- Nakano, S. 2011, Central Bureau Electronic Telegrams, 2892, 1
- Nayak, I., Cenko, S. B., Li, W., et al. 2011, Central Bureau Electronic Telegrams, 2901, 1
- Nishiura, S., Shimada, M., Ohyama, Y., Murayama, T., & Taniguchi, Y. 2000, AJ, 120, 1691
- Ochner, P., Valenti, S., Benetti, S., et al. 2011, Central Bureau Electronic Telegrams, 2873, 2
- Osip, D. J., Phillips, M. M., Bernstein, R., et al. 2004, in Proceedings of the SPIE, Vol. 5492, Society of Photo-Optical Instrumentation Engineers (SPIE) Conference Series, ed. A. F. M. Moorwood & M. Iye, 49–59
- Pastorello, A., Mazzali, P. A., Pignata, G., et al. 2007a, MNRAS, 377, 1531
- Pastorello, A., Taubenberger, S., Elias-Rosa, N., et al. 2007b, MNRAS, 376, 1301
- Perlmutter, S., Aldering, G., Goldhaber, G., et al. 1999, ApJ, 517, 565
- Phillips, M. M. 1993, ApJ, 413, L105
- . 2012, PASA, 29, 434
- Phillips, M. M., Lira, P., Suntzeff, N. B., et al. 1999, AJ, 118, 1766
- Phillips, M. M., Krisciunas, K., Suntzeff, N. B., et al. 2006, AJ, 131, 2615
- Radburn-Smith, D. J., Lucey, J. R., & Hudson, M. J. 2004, MNRAS, 355, 1378
- Riess, A. G., Filippenko, A. V., Challis, P., et al. 1998, AJ, 116, 1009
- Rigault, M., Copin, Y., Aldering, G., et al. 2013, ArXiv e-prints, 1309.1182, arXiv:1309.1182
- Scolnic, D. M., Riess, A. G., Foley, R. J., et al. 2013, ArXiv e-prints, 1306.4050, arXiv:1306.4050

- Skrutskie, M. F., Cutri, R. M., Stiening, R., et al. 2006, *AJ*, 131, 1163
- Stanishev, V., Goobar, A., Benetti, S., et al. 2007, *A&A*, 469, 645
- Stritzinger, M. D., Phillips, M. M., Boldt, L. N., et al. 2011, *AJ*, 142, 156
- Sullivan, M., Conley, A., Howell, D. A., et al. 2010, *MNRAS*, 406, 782
- Wang, X., Wang, L., Pain, R., Zhou, X., & Li, Z. 2006, *ApJ*, 645, 488
- Wang, X., Filippenko, A. V., Ganeshalingam, M., et al. 2009, *ApJ*, 699, L139
- Wood-Vasey, W. M., Miknaitis, G., Stubbs, C. W., et al. 2007, *ApJ*, 666, 694
- Wood-Vasey, W. M., Friedman, A. S., Bloom, J. S., et al. 2008, *ApJ*, 689, 377
- Zhang, T., Chen, J., Wang, X., Lin, L., & Kong, X. 2011a, *Central Bureau Electronic Telegrams*, 2871, 4
- Zhang, T.-M., Zhang, J.-J., & Wang, X.-F. 2011b, *Central Bureau Electronic Telegrams*, 2901, 2

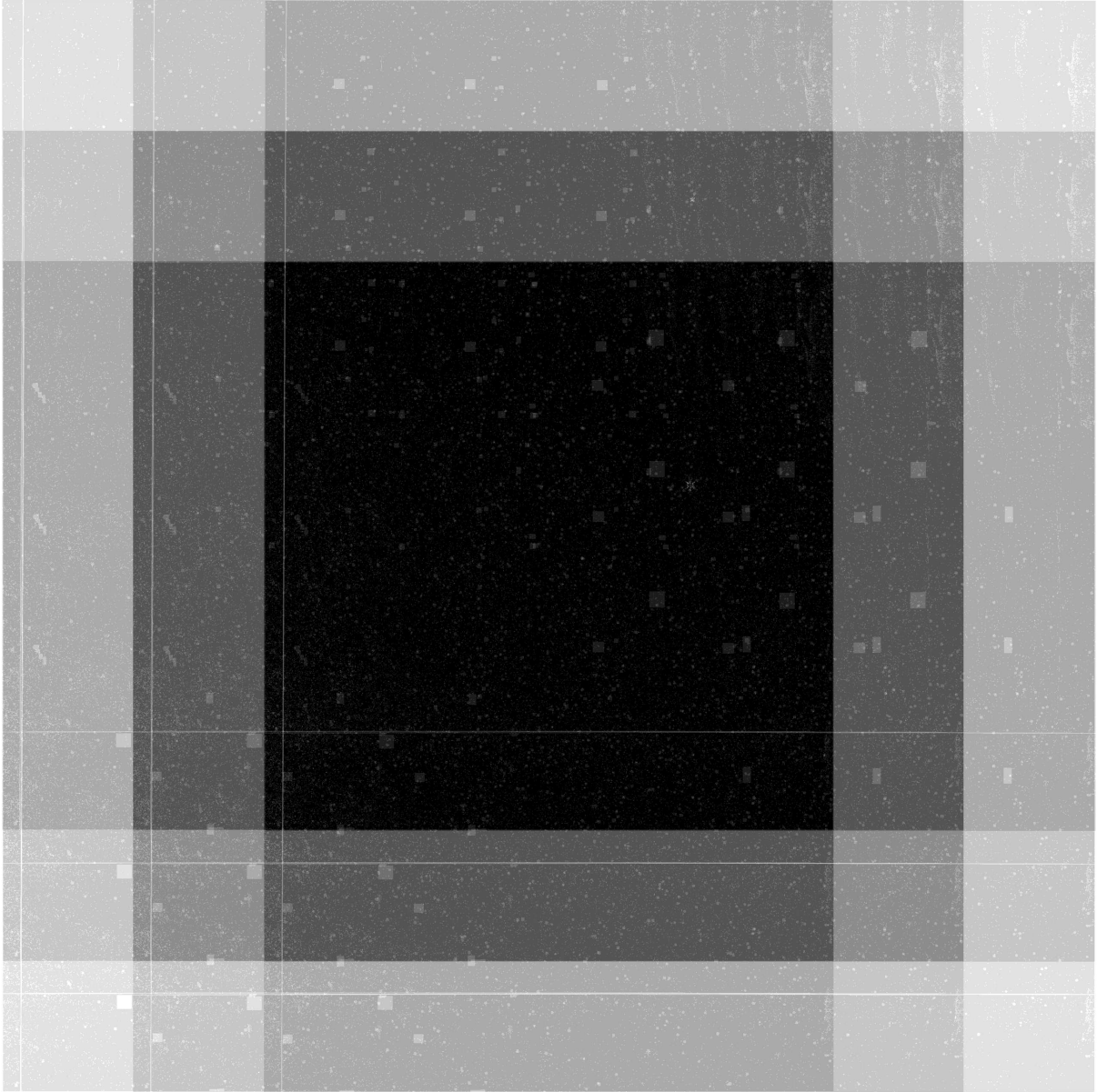


Fig. 1.— Exposure map of a typical stacked observation sequence consisting of a 3x3 grid dither pattern with $30''$ spacing with a 60 s exposure time at each pointing.

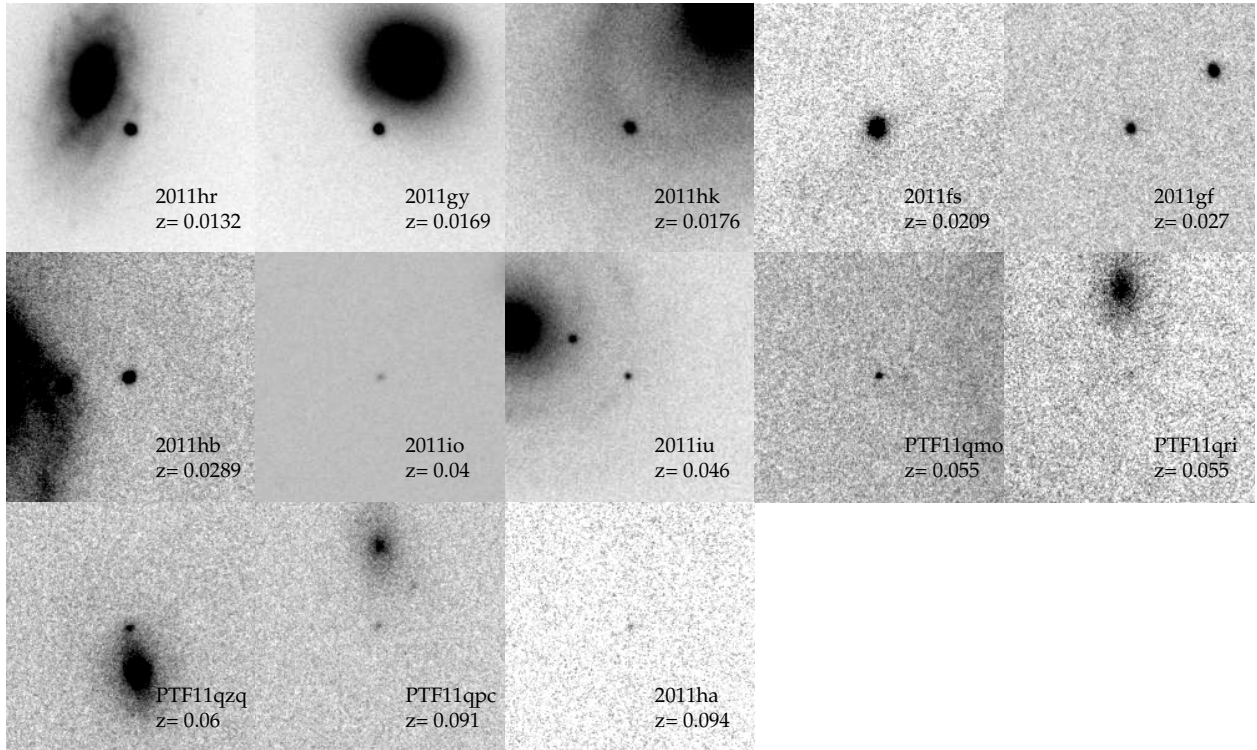


Fig. 2.— Postage stamps of each of the new SNe Ia presented in this work from our WIYN+WHIRC H -band stacked images. The postage stamps are in order of increasing redshift. Each image is $10''$ square.

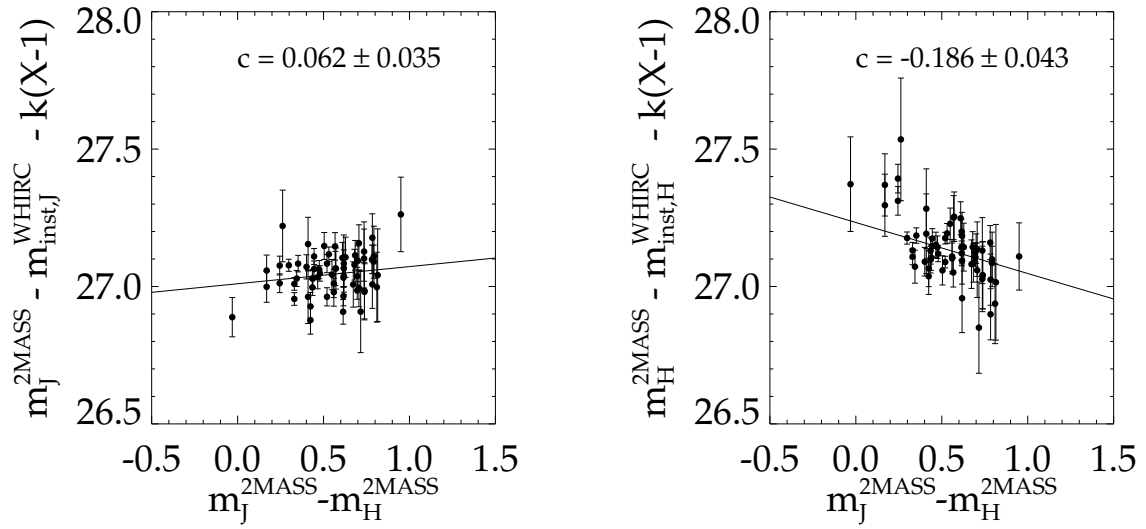


Fig. 3.— The difference in 2MASS magnitude and WHIRC instrumental magnitude corrected for airmass as a function of 2MASS color for the J and H filters. Fitting Eq. 1 to these stars (over-plotted) reveals a significant color term between WHIRC and 2MASS. The results of this fit allow us to transform between the WHIRC and 2MASS system and are used to define our natural WHIRC system.

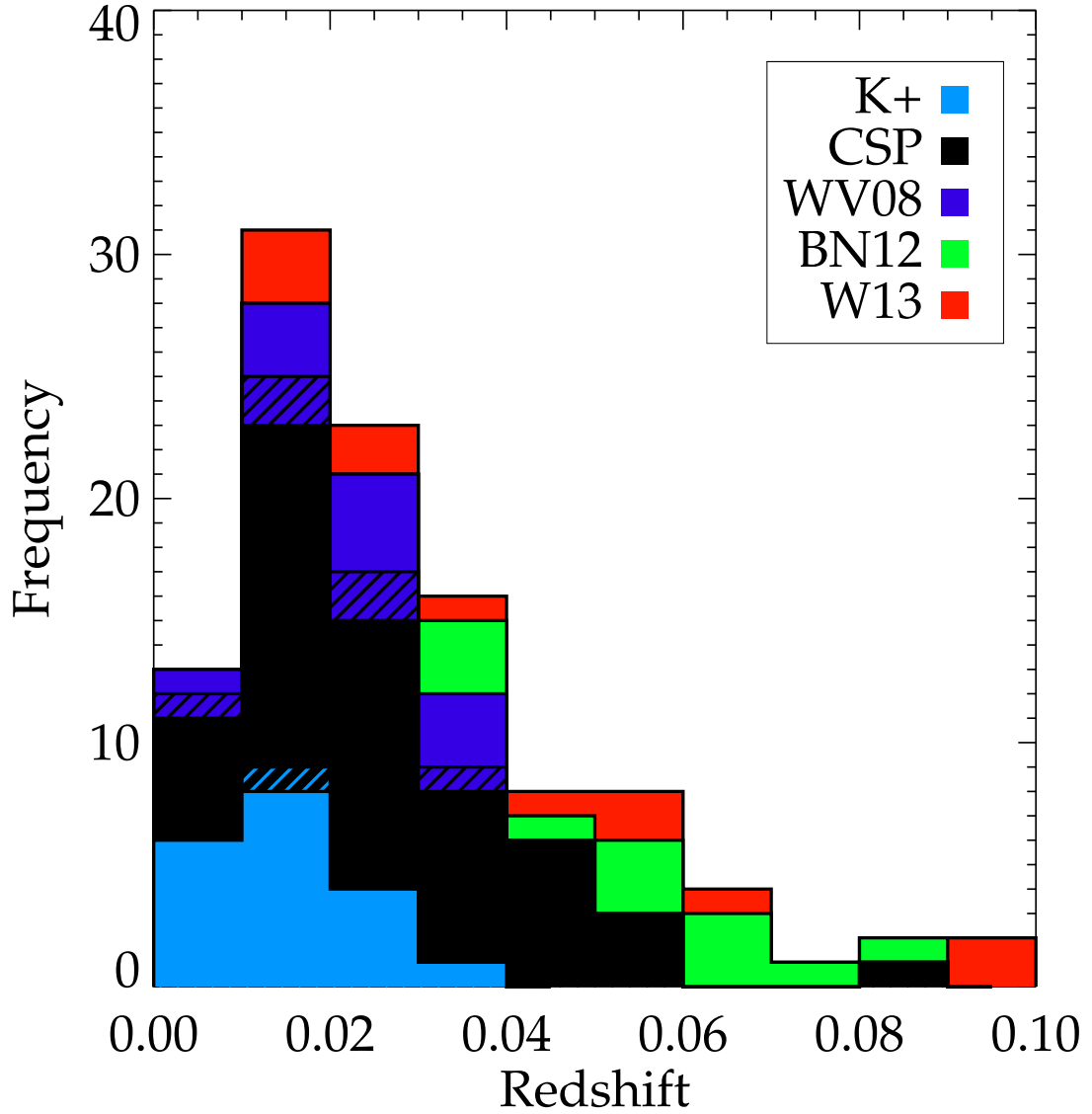


Fig. 4.— Cumulative distribution in redshift of supernovae from the K+ sample in cyan, Contreras et al. (2010) and Stritzinger et al. (2011) in black (CSP), Wood-Vasey et al. (2008) in blue (WV08), Barone-Nugent et al. (2012) in green (BN12), and this present paper in red (W13). The hatched region represents SN observed by multiple groups. With WIYN+WHIRC we can probe a large redshift range and populate the NIR Hubble diagram above $z > 0.03$ where measurements of the distance-redshift relation are less affected by peculiar velocities.

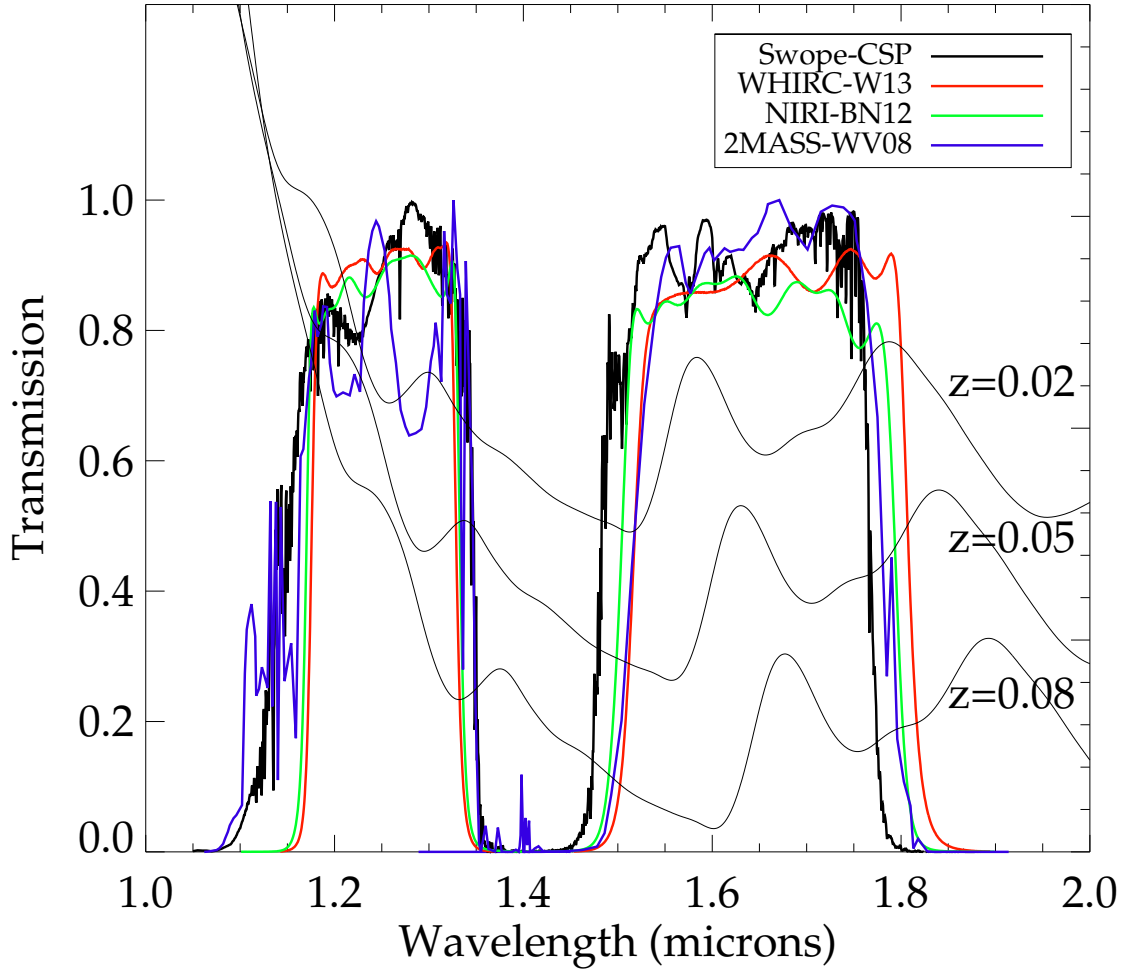


Fig. 5.— Filter transmission for the different instruments in our sample. The atmosphere is included in the filter transmission curve for 2MASS and Swope, but not in the ones for WHIRC and NIRI. Over-plotted is a synthetic spectrum for a Type Ia which is 30 days old from Hsiao et al. (2007) at three different redshifts. Note in particular the variation in the red edge of the filters for the different telescope+detector systems and the shifting of a significant NIR feature (restframe $\lambda \sim 1.75 \mu\text{m}$) from $z = 0.02$ to $z = 0.08$.

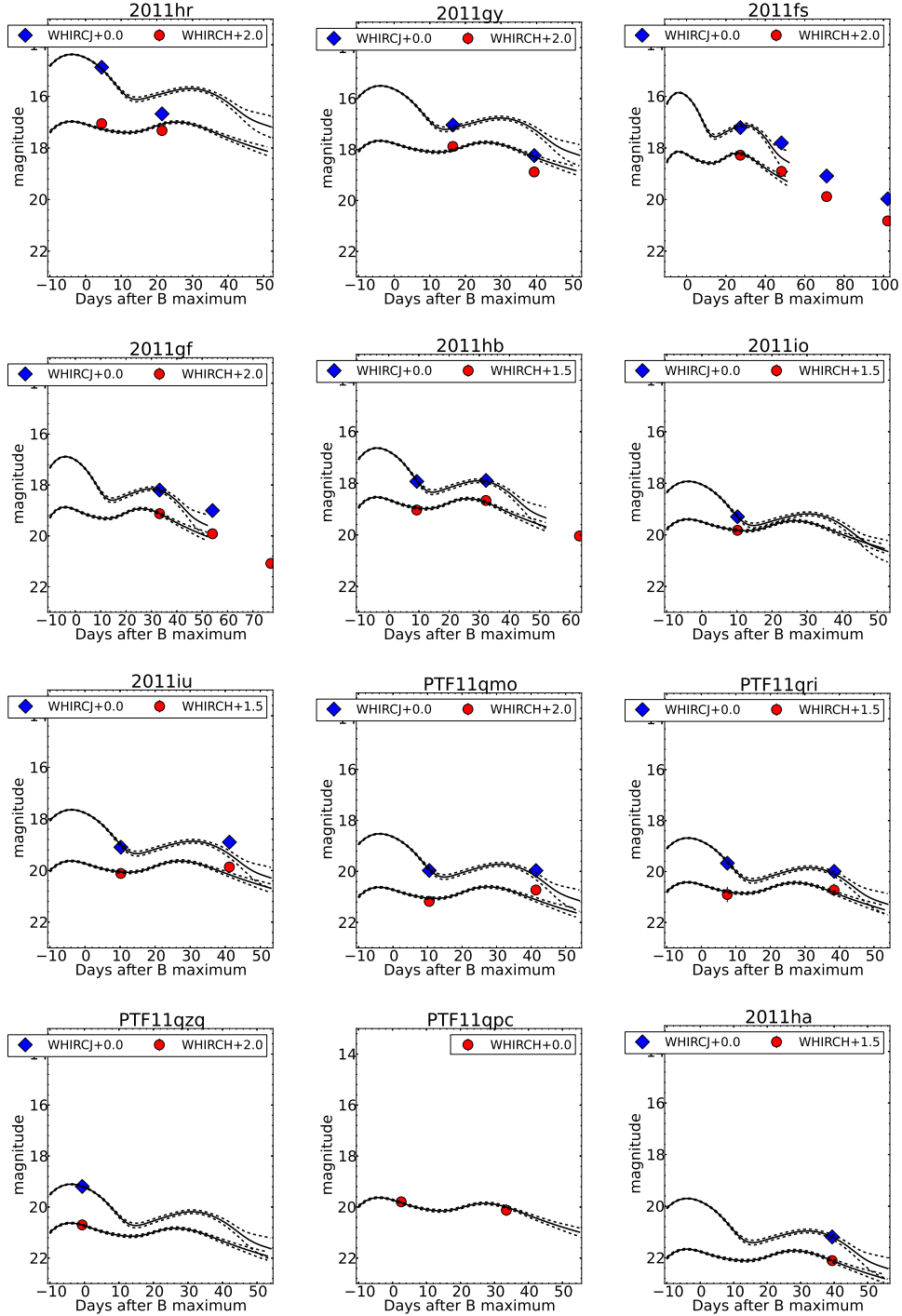


Fig. 6.— SNOoPy light-curve fits for our 12 normal SNe Ia to our H -band (red circle) and J -band (blue diamond) data. H -band is offset for clarity. For these fits the time of maximum was fixed to the value estimated from the spectrum that was used to type the event and was reported in an ATel or CBET. The decline-rate parameter is also fixed to $\Delta m_{15} = 1.1$ making apparent magnitude the only free parameter in the fit. SN 2011hk is not included because it was spectroscopically classified as a sub-luminous supernova similar to SN 1991bg.

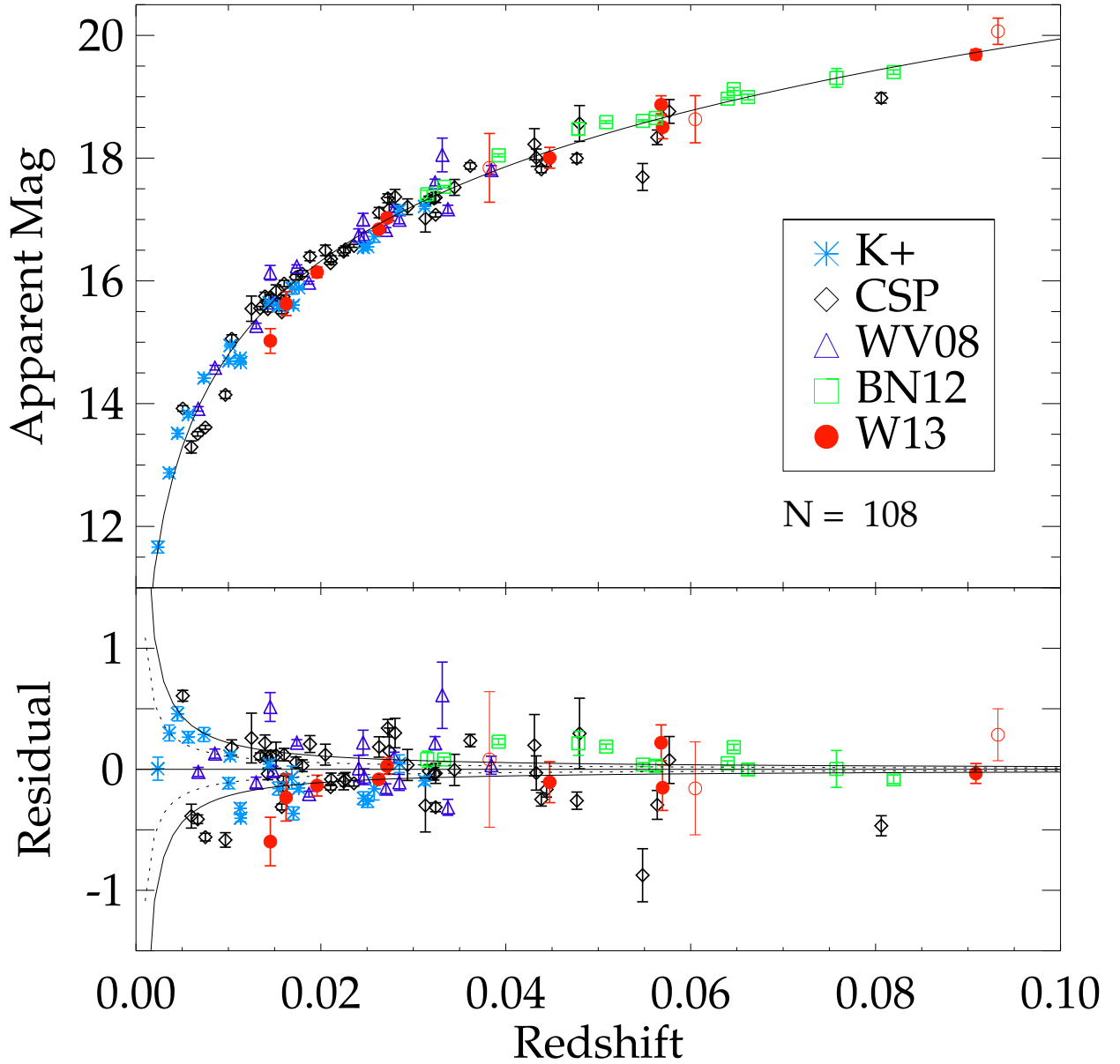


Fig. 7.— (Top) H -band Hubble diagram. The additional supernovae from this work (red circles) confirm the standard nature of SNe Ia in H -band and include the two farthest SNe Ia observed in rest-frame H to date. The open red circles indicate supernovae from our sample which have only one observation in their light curve. The model line plotted over the data is a standard flat LCDM cosmology with $\Omega_M = 0.28$. Assuming a value of $H_0 = 72 \text{ km s}^{-1} \text{ Mpc}^{-1}$ we measure the SN Ia H -band absolute magnitude from the entire sample to be $-18.314 \pm 0.024 \text{ mag}$. (Bottom) Hubble residuals (data–model). The solid (dotted) line represents the magnitude associated with a peculiar velocity uncertainty in redshift of 300 km s^{-1} (150 km s^{-1}). Note that the largest statistical outlier from our sample, SN 2011hr, is both the lowest-redshift of our sample ($z = 0.01328$) and is also spectroscopically classified as 91T-like and could be expected to be over-luminous with respect to the assumption of a fiducial SN Ia made in our fits.

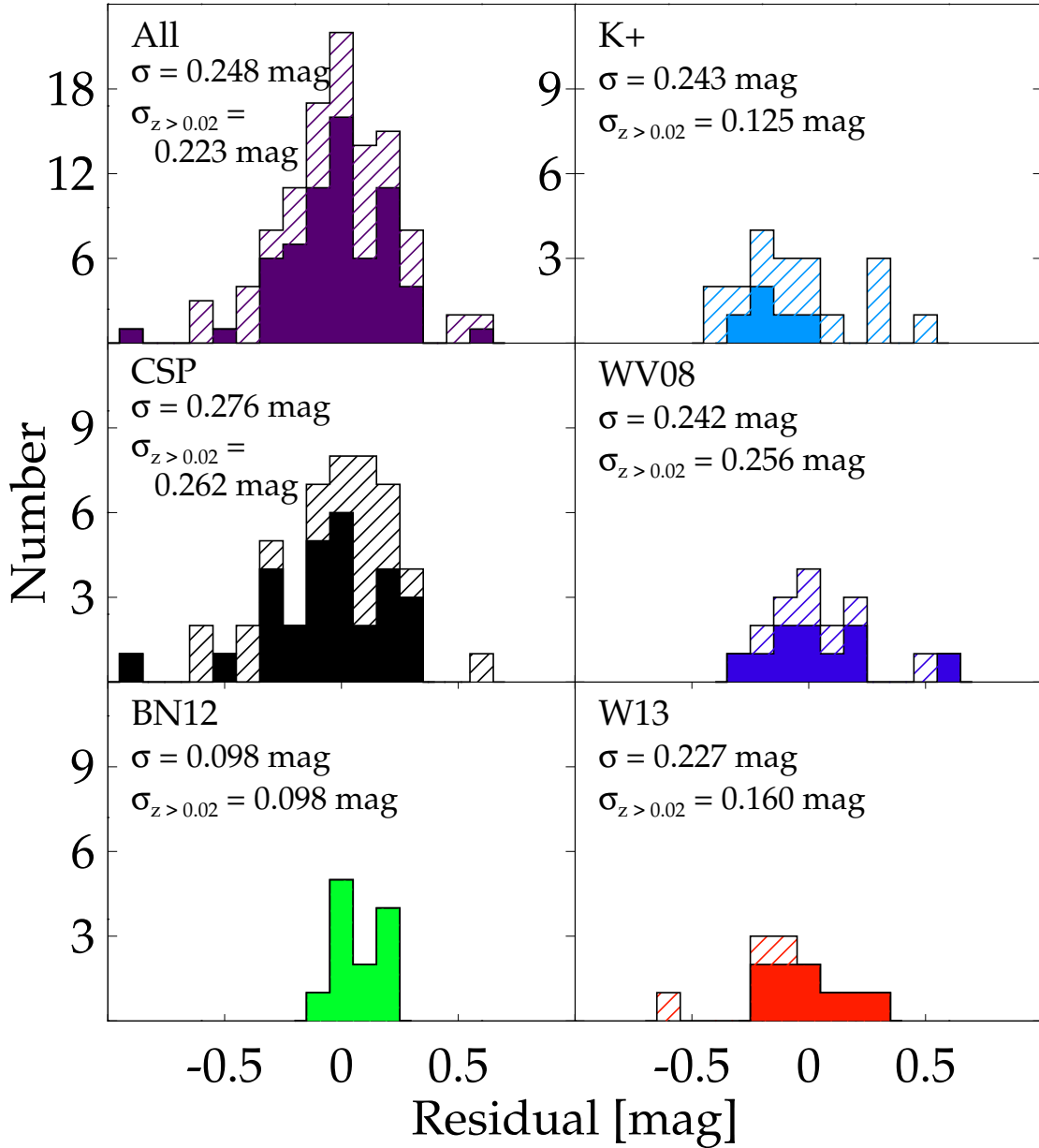


Fig. 8.— Distribution of the H-band residuals with respect to the global mean -18.314 ± 0.024 mag, organized by survey for the entire sample (hatched) and for SN Ia with $z > 0.02$ (solid). Supernovae observed by WV08 and CSP are included in the WV08 sample. The weighted standard deviation is quoted in the top right corner for the whole sample (top) and the higher redshift sub-sample (bottom). One can clearly see the benefit of obtaining a sample in the smooth Hubble flow by the tight BN12 residual distribution and to some extent in W13.

Table 1. SN Ia Properties

SN	Host Galaxy	Spectral ^a Subtype	ATel/CBET	Discovery Group ^b / Individual	Disc./Spec. ^c Reference
SN 2011hr	NGC 2691	91T-like	CBET 2901	LOSS	N11, Z11b
SN 2011gy	UGC 02756	Normal	CBET 2871	Z. Jin, X. Goa	JG11, Z11a
SN 2011hk	NGC 0881	91bg-like	CBET 2892	K. Itagaki, Y. Hirose	Na11, MB11b
			ATEL 3798	PTF	GY11b
SN 2011fs	UGC 11975	Normal	CBET 2825	Z. Jin, X. Goa	J11, B11
SN 2011gf	SDSS J211222.69-074913.9	Normal	CBET 2838	CRTS	D11, M11
SN 2011hb	NGC 7674	Normal	CBET 2880	CRTS	H11, MB11a
			ATEL 3739	PTF	GY11a
SN 2011io	2MASX J23024668+0848186	Normal	CBET 2931	MASTER	BL11, F11
SN 2011iu	UGC 12809	Normal	CBET 2939	Puckett	C11, MB11c
PTF11qri	LCRS B124431.1-060321	SN Ia	ATEL 3798	PTF	GY11b
PTF11qmo	2MASX J10064866-0741124	SN Ia	ATEL 3798	PTF	GY11b
PTF11qzq	2MASX J07192718+5413454	SN Ia	ATEL 3798	PTF	GY11b
PTF11qpc	SDSS J122005.46+092418.3	SN Ia	ATEL 3798	PTF	GY11b
SN 2011ha	PGC 1375631	Normal	CBET 2873	MASTER	LB11, O11

^aSpectral classifications according to SNID (Blondin & Tonry 2007) and PTF. Subtypes given when provided in the original CBET or ATEL.

^bReferences/URLs: KAIT/LOSS (Filippenko et al. 2001); CRTS (Drake et al. 2009); PTF <http://www.astro.caltech.edu/ptf/>; MASTER http://observ.pereplet.ru/sn_e.html; Puckett <http://www.cometwatch.com>

^cReference Codes: N11: Nayak et al. (2011); Z11b: Zhang et al. (2011b); JG11: Jin & Gao (2011); Z11a: Zhang et al. (2011a); Na11: Nakano (2011); MB11b: Marion & Berlind (2011b); GY11b: Gal-Yam et al. (2011a); J11: Jin et al. (2011); B11: Balam et al. (2011); D11: Drake et al. (2011); M11: Marion (2011); H11: Howerton et al. (2011); MB11a: Marion & Berlind (2011a); GY11a: Gal-Yam et al. (2011b); BL11: Balanutsa & Lipunov (2011); F11: Fraser et al. (2011); C11: Cox et al. (2011); MB11c: Marion & Berlind (2011c); LB11: Lipunov & Balanutsa (2011); O11: Ochner et al. (2011)

Table 2. SN Ia Sample Summary I

Name	RA(J2000)	Dec(J2000)	t_{\max}^a	z_{helio}	z from Host or SN	Redshift Citation
SN 2011hr	08:54:46.03	+39:32:16.1	55883	0.01328	Host	de Vaucouleurs et al. (1991) ^b
SN 2011gy	03:29:35.30	+40:52:02.9	55865	0.01688	Host	Falco et al. (1999) ^b
SN 2011hk	02:18:45.84	-06:38:30.3	...	0.01756	Host	Bottinelli et al. (1993) ^b
SN 2011fs	22:17:19.52	+35:34:50.0	55833	0.02091	Host	Fisher et al. (1995) ^b
SN 2011gf	21:12:24.27	-07:48:52.0	55827	0.02766	Host	Abazajian et al. (2003) ^b
SN 2011hb	23:27:55.52	+08:46:45.0	55872	0.02892	Host	Nishiura et al. (2000) ^b
SN 2011io	23:02:47.59	+08:48:09.8	55894	0.04	SN	Fraser et al. (2011)
SN 2011iu	23:51:02.27	+46:43:21.7	55894	0.04598	Host	Bottinelli et al. (1993) ^b
PTF11qri	12:47:06.28	-06:19:49.7	55897	0.055	SN	Gal-Yam et al. (2011a)
PTF11qmo	10:06:49.76	-07:41:12.3	55894	0.05523	Host	Jones et al. (2009) ^b
PTF11qzq	07:19:27.24	+54:13:48.0	55905	0.06	SN	Gal-Yam et al. (2011a)
PTF11qpc	12:20:05.47	+09:24:12.1	55902	0.08902	Host	Abazajian et al. (2005) ^b
SN 2011ha	03:57:40.87	+10:09:55.2	55842	0.094	SN	Ochner et al. (2011)

^aTime of maximum in the B -band according to SNID/PTF reported in CBET/ATel.

^bHeliocentric redshifts citations via NASA/IPAC Extragalactic Database (NED) <http://ned.ipac.caltech.edu/>.

Table 3. SN Ia Sample Summary II

Name	$z_{\text{CMB+VIRGO}}^a$	nobs _J	nobs _H	$m_{J,\max}$ [mag]	$\sigma(m_{J,\max})^b$ [mag]	$m_{H,\max}$ [mag]	$\sigma(m_{H,\max})^b$ [mag]
SN 2011hr	0.01453	2	2	14.352	0.220	15.022	0.200
SN 2011gy	0.01623	2	2	15.300	0.285	15.630	0.194
SN 2011hk	0.01625	2	2
SN 2011fs	0.01958	4	4	15.727	0.123	16.141	0.085
SN 2011gf	0.02626	2	3	16.814	0.020	16.841	0.010
SN 2011hb	0.02715	2	3	16.623	0.105	17.026	0.068
SN 2011io	0.04 ± 0.01	1	1	17.817	0.558	17.841	0.560
SN 2011iu	0.04475	2	2	17.640	0.232	18.005	0.169
PTF11qri	0.057 ± 0.001	2	2	18.769	0.122	18.689	0.147
PTF11qmo	0.05696	2	2	18.621	0.265	18.503	0.188
PTF11qzq	0.06 ± 0.01	1	1	19.122	0.377	18.634	0.383
PTF11qpc	0.09084	0	2	19.687	0.082
SN 2011ha	0.093 ± 0.001	1	1	19.520	0.152	20.067	0.214

^aWe follow Mould et al. (2000) to correct for the Virgo cluster and transform to the CMB using Karachentsev & Makarov (1996) and Fixsen et al. (1996).

^bError includes photometric and redshift uncertainty as well as uncertainty from the template used to fit the data.

Table 4. Photometric Calibration Terms

Filter	zeropoint [mag]	k [mag/airmass]	c
J	27.041 ± 0.012	-0.051 ± 0.020	$+0.062 \pm 0.035$
H	27.140 ± 0.014	-0.066 ± 0.030	-0.186 ± 0.043

Table 5. 2MASS Calibration Stars

2MASS ID	SN Field	WHIRC Natural System				2MASS Catalog Magnitudes					
		m_J [mag]	$\sigma(m_J)$	m_H [mag]	$\sigma(m_H)$	m_J [mag]	$\sigma(m_J)$ [mag]	m_H [mag]	$\sigma(m_H)$ [mag]	m_{K_s} [mag]	$\sigma(m_{K_s})$ [mag]
2MASS 02184937–0637528	SN 2011hk	15.162	0.021	14.384	0.029	15.022	0.045	14.408	0.047	14.257	0.059
2MASS 03293834+4051347	SN 2011gy	16.640	0.025	15.883	0.040	16.565	0.102	15.827	0.122	15.450	0.123
2MASS 03573901+1009372	SN 2011ha	14.570	0.015	14.119	0.021	14.592	0.033	14.117	0.041	13.925	0.051
2MASS 07192306+5414071	PTF11qzq	16.788	0.022	16.060	0.042	16.725	0.127	15.915	0.145
2MASS 08544039+3933230	SN 2011hr	15.526	0.015	14.923	0.023	15.587	0.054	14.903	0.070	14.738	0.085
2MASS 10064485–0740334	PTF11qmo	16.325	0.022	15.570	0.038	16.376	0.109	15.583	0.099	15.429	0.221
2MASS 12200392+0925144	PTF11qpc	13.728	0.021	14.482	0.036	13.779	0.043	13.526	0.050
2MASS 12470715–0620106	PTF11qri	15.019	0.019	14.770	0.030	15.017	0.029	14.673	0.060	14.757	0.096
2MASS 21122081–0748443	SN 2011gf	15.131	0.020	14.317	0.029	15.171	0.052	14.389	0.062	14.280	0.068
2MASS 22172193+3533349	SN 2011fs	15.708	0.020	15.423	0.032	15.686	0.056	15.517	0.113	15.653	0.244
2MASS 23024227+0848225	SN 2011io	15.875	0.019	15.529	0.030	15.732	0.070	15.163	0.090	14.966	0.128
2MASS 23275179+0846392	SN 2011hb	15.745	0.024	15.021	0.037	15.684	0.067	14.978	0.099	14.838	0.097
2MASS 23505996+4643586	SN 2011iu	15.389	0.018	14.760	0.026	15.379	0.055	14.830	0.057	14.461	0.071

Table 6. SN Ia Light Curves

Name	Date MJD	Filter	m ^a [mag]	$\sigma(m)$ [mag]	Δ_m^{Kcorr} ^b [mag]
SN 2011hr	55887.52	<i>J</i>	14.872	0.024	-0.042
SN 2011hr	55904.47	<i>J</i>	16.676	0.037	0.023
SN 2011hr	55887.52	<i>H</i>	15.056	0.036	-0.073
SN 2011hr	55904.46	<i>H</i>	15.325	0.037	-0.114
SN 2011gy	55881.50	<i>J</i>	17.036	0.040	-0.009
SN 2011gy	55904.32	<i>J</i>	18.237	0.051	-0.017
SN 2011gy	55881.47	<i>H</i>	15.879	0.045	-0.089
SN 2011gy	55904.30	<i>H</i>	16.879	0.057	-0.062
SN 2011hk	55881.36	<i>J</i>	17.572	0.024	...
SN 2011hk	55904.28	<i>J</i>	19.671	0.071	...
SN 2011hk	55881.34	<i>H</i>	17.027	0.033	...
SN 2011hk	55904.26	<i>H</i>	18.415	0.057	...
SN 2011fs	55860.31	<i>J</i>	17.209	0.038	-0.016
SN 2011fs	55881.17	<i>J</i>	17.804	0.029	-0.025
SN 2011fs	55904.12	<i>J</i>	19.087	0.045	-0.016
SN 2011fs	55935.11	<i>J</i>	19.975	0.185	0.000
SN 2011fs	55860.30	<i>H</i>	16.281	0.040	-0.072
SN 2011fs	55881.16	<i>H</i>	16.908	0.035	-0.063
SN 2011fs	55904.10	<i>H</i>	17.886	0.044	-0.063
SN 2011fs	55935.08	<i>H</i>	18.829	0.135	0.000
SN 2011gf	55860.22	<i>J</i>	18.200	0.044	-0.065
SN 2011gf	55881.08	<i>J</i>	19.004	0.046	-0.066
SN 2011gf	55860.23	<i>H</i>	17.126	0.045	-0.042
SN 2011gf	55881.07	<i>H</i>	17.917	0.052	-0.054
SN 2011gf	55904.07	<i>H</i>	19.081	0.188	0.000
SN 2011hb	55881.29	<i>J</i>	17.927	0.035	-0.083
SN 2011hb	55904.20	<i>J</i>	17.888	0.025	-0.072
SN 2011hb	55881.28	<i>H</i>	17.536	0.043	-0.032
SN 2011hb	55904.18	<i>H</i>	17.166	0.038	-0.034
SN 2011hb	55935.14	<i>H</i>	18.542	0.111	-0.048
SN 2011io	55904.16	<i>J</i>	19.172	0.058	-0.124
SN 2011io	55904.14	<i>H</i>	18.343	0.055	0.020
SN 2011iu	55904.24	<i>J</i>	19.096	0.033	-0.141
SN 2011iu	55935.20	<i>J</i>	18.899	0.114	-0.198
SN 2011iu	55904.22	<i>H</i>	18.612	0.038	0.047
SN 2011iu	55935.18	<i>H</i>	18.362	0.104	-0.060
PTF11qri	55904.54	<i>J</i>	19.672	0.129	-0.147
PTF11qri	55935.47	<i>J</i>	19.992	0.146	-0.268
PTF11qri	55904.52	<i>H</i>	19.402	0.301	0.027
PTF11qri	55935.45	<i>H</i>	19.224	0.251	-0.039

Table 6—Continued

Name	Date MJD	Filter	m ^a [mag]	$\sigma(m)$ [mag]	Δ_m^{Kcorr} ^b [mag]
PTF11qmo	55904.50	<i>J</i>	19.963	0.075	-0.175
PTF11qmo	55935.42	<i>J</i>	19.966	0.163	-0.275
PTF11qmo	55904.49	<i>H</i>	19.176	0.068	0.083
PTF11qmo	55935.39	<i>H</i>	18.729	0.099	-0.058
PTF11qzq	55904.36	<i>J</i>	19.056	0.043	-0.136
PTF11qzq	55904.34	<i>H</i>	18.635	0.078	-0.065
PTF11qpc	55904.56	<i>H</i>	19.795	0.108	-0.079
PTF11qpc	55935.50	<i>H</i>	20.122	0.225	0.126
SN 2011ha	55881.40	<i>J</i>	20.434	0.130	-0.756
SN 2011ha	55881.38	<i>H</i>	20.627	0.191	0.018

^aMagnitudes reported in the WHIRC natural system, which is referenced to 2MASS at $(m_J^{2\text{MASS}} - m_H^{2\text{MASS}}) = 0.5$ mag.

^bK-correction as calculated by SNooPY (Burns et al. 2011). Subtract K-correction value (column 6) from reported natural-system magnitude (column 4) to yield K-corrected magnitude in the CSP system (Stritzinger et al. 2011).

Table 7. H -band Maximum Apparent Magnitude for Current Sample

Name	t_{\max}^a	z_{CMB}	$\sigma(z_{\text{CMB}})$	$m_{H,\max}$ [mag]	$\sigma(m_{H,\max})$ [mag]	Reference ^b	Sample ^c
SN 1998bu	50953.4	0.0024	0.0001	11.662	0.025	J99,H00	K+
SN 1999cp	51364.2	0.0113	0.0001	14.741	0.039	K00	K+
SN 1999ee	51470.1	0.0102	0.0001	14.948	0.017	K04a	K+
SN 1999ek	51482.5	0.0176	0.0001	15.885	0.027	K04b	K+
SN 1999gp	51550.7	0.0258	0.0001	16.722	0.093	K01	K+
SN 2000E	51577.5	0.0045	0.0001	13.516	0.033	V03	K+
SN 2000bh	51634.5	0.0246	0.0001	16.541	0.054	K04a	K+
SN 2000bk	51645.7	0.0285	0.0001	17.151	0.072	K01	K+
SN 2000ca	51667.7	0.0251	0.0001	16.556	0.048	K04a	K+
SN 2000ce	51670.6	0.0169	0.0001	15.878	0.094	K01	K+
SN 2001ba	52035.3	0.0312	0.0001	17.212	0.034	K04a	K+
SN 2001bt	52064.1	0.0144	0.0001	15.643	0.030	K04a	K+
SN 2001cn	52072.6	0.0154	0.0001	15.591	0.053	K04b	K+
SN 2001cz	52104.9	0.0170	0.0001	15.603	0.053	K04b	K+
SN 2001el	52182.3	0.0036	0.0001	12.871	0.025	K03	K+
SN 2002bo	52357.3	0.0057	0.0001	13.822	0.026	K04b	K+
SN 2002dj	52450.8	0.0113	0.0001	14.669	0.021	P08	K+
SN 2003du	52768.2	0.0074	0.0001	14.417	0.050	St07	K+
SN 2004S	53040.2	0.0100	0.0001	14.693	0.040	K07	K+
SN 2004ef	53264.5	0.0294	0.0001	17.208	0.128	C10	CSP
SN 2004eo	53278.5	0.0146	0.0001	15.692	0.043	Pa07b,C10	CSP
SN 2004ey	53304.9	0.0143	0.0001	15.672	0.022	C10	CSP
SN 2004gs	53354.7	0.0280	0.0001	17.369	0.122	C10	CSP
SN 2004gu	53366.1	0.0477	0.0001	17.995	0.071	C10	CSP
SN 2005M	53406.2	0.0236	0.0001	16.570	0.022	C10	CSP
SN 2005ag	53415.1	0.0806	0.0001	18.980	0.083	C10	CSP
SN 2005al	53430.1	0.0140	0.0001	15.749	0.064	C10	CSP
SN 2005am	53435.1	0.0097	0.0001	14.144	0.056	C10	CSP
SN 2005ao	53441.2	0.0384	0.0001	17.805	0.075	WV08	WV08
SN 2005cf	53534.0	0.0067	0.0001	13.914	0.018	WV08,Pa07a	WV08
SN 2005ch	53535.0	0.0285	0.0001	16.996	0.066	WV08	WV08
SN 2005el	53648.2	0.0148	0.0001	15.647	0.039	WV08,C10	WV08
SN 2005eq	53655.9	0.0279	0.0001	17.159	0.042	WV08,C10	WV08
SN 2005eu	53665.8	0.0337	0.0001	17.167	0.066	WV08	WV08
SN 2005hc	53668.2	0.0444	0.0001	17.929	0.063	C10	CSP
SN 2005hj	53675.8	0.0564	0.0001	18.338	0.119	S11	CSP
SN 2005iq	53687.4	0.0323	0.0001	17.603	0.054	WV08,C10	WV08
SN 2005kc	53698.2	0.0134	0.0001	15.555	0.024	C10	CSP
SN 2005ki	53705.8	0.0211	0.0001	16.359	0.051	C10	CSP
SN 2005na	53741.3	0.0270	0.0001	16.829	0.040	WV08,C10	WV08

Table 7—Continued

Name	t_{\max}^a	z_{CMB}	$\sigma(z_{\text{CMB}})$	$m_{H,\max}$ [mag]	$\sigma(m_{H,\max})$ [mag]	Reference ^b	Sample ^c
SN 2006D	53757.0	0.0085	0.0001	14.585	0.028	WV08,C10	WV08
SN 2006N	53759.2	0.0145	0.0001	16.132	0.118	WV08	WV08
SN 2006ac	53781.2	0.0247	0.0001	16.725	0.065	WV08	WV08
SN 2006ax	53827.5	0.0187	0.0001	15.971	0.021	WV08,C10	WV08
SN 2006bh	53833.4	0.0104	0.0001	15.058	0.059	C10	CSP
SN 2006br	53851.4	0.0263	0.0001	17.112	0.084	S11	CSP
SN 2006cp	53897.2	0.0241	0.0001	16.740	0.108	WV08	WV08
SN 2006ej	53975.1	0.0188	0.0001	16.397	0.069	S11	CSP
SN 2006eq	53971.4	0.0480	0.0001	18.564	0.292	C10	CSP
SN 2006et	53994.7	0.0210	0.0001	16.288	0.021	S11	CSP
SN 2006ev	53987.4	0.0272	0.0001	17.346	0.072	S11	CSP
SN 2006gj	53998.3	0.0274	0.0001	17.169	0.190	S11	CSP
SN 2006gr	54012.9	0.0331	0.0001	18.052	0.274	WV08	WV08
SN 2006gt	54000.1	0.0431	0.0001	18.226	0.254	C10	CSP
SN 2006hb	53997.3	0.0152	0.0001	15.828	0.107	S11	CSP
SN 2006hx	54022.6	0.0438	0.0001	17.817	0.055	S11	CSP
SN 2006is	53996.1	0.0313	0.0001	17.016	0.219	S11	CSP
SN 2006kf	54040.4	0.0205	0.0001	16.497	0.086	S11	CSP
SN 2006le	54048.1	0.0174	0.0001	16.234	0.023	WV08	WV08
SN 2006lf	54045.7	0.0130	0.0001	15.265	0.042	WV08	WV08
SN 2006lu	54037.9	0.0548	0.0001	17.693	0.219	S11	CSP
SN 2006ob	54062.0	0.0577	0.0001	18.761	0.194	S11	CSP
SN 2006os	54064.6	0.0317	0.0001	17.326	0.052	S11	CSP
SN 2007A	54113.9	0.0160	0.0001	15.957	0.049	S11	CSP
SN 2007S	54145.4	0.0158	0.0001	15.489	0.020	S11	CSP
SN 2007af	54174.8	0.0075	0.0001	13.613	0.013	S11	CSP
SN 2007ai	54174.8	0.0324	0.0001	17.078	0.036	S11	CSP
SN 2007as	54181.3	0.0180	0.0001	16.119	0.047	S11	CSP
SN 2007bc	54201.3	0.0226	0.0001	16.514	0.056	S11	CSP
SN 2007bd	54207.6	0.0322	0.0001	17.343	0.052	S11	CSP
SN 2007ca	54228.5	0.0159	0.0001	15.666	0.029	S11	CSP
SN 2007cq	54280.6	0.0246	0.0001	16.998	0.102	WV08	WV08
SN 2007jg	54366.6	0.0362	0.0001	17.873	0.051	S11	CSP
SN 2007le	54399.8	0.0051	0.0001	13.922	0.013	S11	CSP
SN 2007nq	54396.5	0.0433	0.0001	18.008	0.141	S11	CSP
SN 2007on	54419.8	0.0060	0.0001	13.293	0.092	S11	CSP
SN 2008C	54466.6	0.0173	0.0001	16.062	0.043	S11	CSP
SN 2008R	54490.6	0.0125	0.0001	15.547	0.205	S11	CSP
SN 2008bc	54550.7	0.0160	0.0001	15.744	0.023	S11	CSP
SN 2008bq	54564.6	0.0345	0.0001	17.523	0.129	S11	CSP

Table 7—Continued

Name	t_{\max}^a	z_{CMB}	$\sigma(z_{\text{CMB}})$	$m_{H,\max}$ [mag]	$\sigma(m_{H,\max})$ [mag]	Reference ^b	Sample ^c
SN 2008fp	54731.7	0.0067	0.0001	13.507	0.014	S11	CSP
SN 2008gp	54779.9	0.0324	0.0001	17.359	0.082	S11	CSP
SN 2008hv	54817.6	0.0143	0.0001	15.541	0.046	S11	CSP
SN 2008ia	54813.0	0.0225	0.0001	16.477	0.066	S11	CSP
PTF09dlc	55073.7	0.0662	0.0001	18.995	0.046	BN12	BN12
PTF10hdv	55344.1	0.0548	0.0001	18.608	0.016	BN12	BN12
PTF10hmv	55351.4	0.0333	0.0001	17.534	0.018	BN12	BN12
PTF10mwb	55390.7	0.0315	0.0001	17.412	0.066	BN12	BN12
PTF10ndc	55390.3	0.0820	0.0001	19.402	0.036	BN12	BN12
PTF10nlg	55391.5	0.0562	0.0001	18.655	0.040	BN12	BN12
PTF10qyx	55426.1	0.0647	0.0001	19.125	0.024	BN12	BN12
PTF10tce	55442.0	0.0392	0.0001	18.045	0.023	BN12	BN12
PTF10ufj	55456.5	0.0758	0.005	19.307	0.035	BN12	BN12
PTF10wnm	55476.5	0.0640	0.0001	18.969	0.019	BN12	BN12
PTF10wof	55474.2	0.0508	0.0001	18.587	0.020	BN12	BN12
PTF10xyt	55490.9	0.0478	0.0001	18.477	0.099	BN12	BN12
PTF11qmo	55894	0.05696	0.0001	18.503	0.188	W13	W13
PTF11qpc	55902	0.09084	0.0001	19.687	0.082	W13	W13
PTF11qri	55897	0.057	0.001	18.689	0.147	W13	W13
PTF11qzq	55905	0.06	0.01	18.634	0.383	W13	W13
SN 2011fs	55833	0.01958	0.0001	16.141	0.085	W13	W13
SN 2011gf	55827	0.02626	0.0001	16.841	0.010	W13	W13
SN 2011gy	55865	0.01623	0.0001	15.630	0.194	W13	W13
SN 2011ha	55842	0.093	0.001	20.067	0.214	W13	W13
SN 2011hb	55872	0.02715	0.0001	17.026	0.068	W13	W13
SN 2011hr	55883	0.01453	0.0001	15.022	0.200	W13	W13
SN 2011io	55894	0.04	0.01	17.841	0.560	W13	W13
SN 2011iu	55894	0.04475	0.0001	18.005	0.169	W13	W13

^a t_{\max} from B -band optical light curve fits using SNoopy for WV08 and CSP and reported B -band t_{\max} from Maguire et al. (2012) for BN12.

^bReference codes J99: Jha et al. (1999); H00: Hernandez et al. (2000); K00: Krisciunas et al. (2000); K04a: Krisciunas et al. (2004a); K04b: Krisciunas et al. (2004b); Ph06: Phillips et al. (2006); Pa07a: Pastorello et al. (2007b); Pa07b: Pastorello et al. (2007a); St07: Stanishev et al. (2007); WV08: Wood-Vasey et al. (2008); C10: Contreras et al. (2010); S11: Stritzinger et al. (2011); BN12: Barone-Nugent et al. (2012); W13: this present paper.

^cSample name used for the divisions in the analysis. Some SNe Ia were observed by multiple projects. We assign each SNe Ia to a single sample for the purposes of quoting dispersions and distributions in the analysis.